https://doi.org/10.5194/egusphere-2024-1758
Preprint. Discussion started: 20 June 2024

Evaluating state-of-the-art process-based and data-driven models in simulating CO_2 fluxes and their relationship with climate in western European temperate forests

Gaïa Michel[1,2], Julien Crétat[1], Olivier Mathieu[1], Mathieu Thévenot[1], Andrey Dara[3], Robert Granat[3], Zhendong Wu[4,5], Clément Bonnefoy-Claudet[1], Julianne Capelle[1], Jean Cacot[6], John S. Kimball[7]

[1] Biogéosciences, UMR 6282 CNRS, Université de Bourgogne, Dijon, France
[2] AgroParisTech, 91120, Palaiseau, France
[3] CarbonSpace Ltd., D04H1F3 Dublin, Ireland
[4] Department of Physical Geography and Ecosystem Science, Lund University, Lund, Sweden
[5] ICOS ERIC, Carbon Portal, Lund, Sweden
[6] Centre National de la Propriété Forestière, Saulieu, France
[7] Numerical Terradynamic Simulation Group, University of Montana, Missoula, MT, United States of America

Correspondence to: Julien Crétat (julien.cretat@u-bourgogne.fr)

https://doi.org/10.5194/egusphere-2024-1758
Preprint. Discussion started: 20 June 2024

Abstract.

This study evaluates two process-based (LPJ-GUESS and SMAP-L4C) and two data-driven (CarbonSpace and FLUXCOM) models to capture the temporal variability of CO_2 flux exchanges (GPP, RECO and NEE) of evergreen needleleaf and deciduous broadleaf forests (ENFs and DBFs) in temperate western Europe and its relationship with climate. Three sites from the FLUXNET network are considered together with two non-instrumented sites located in Burgundy (North-East France). The focus is put on the representation of the annual cycle, annual budget, interannual variability and "long-term" trend. The data-driven models are the best models for representing the mean annual cycle and mean annual budget in CO_2 fluxes despite magnitude uncertainties. In particular, the models accounting for plant functional types in their outputs tend to simulate more marked annual cycle and lower annual CO_2 sequestration for DBFs than ENFs in Burgundy. At the interannual timescale, the CO_2 flux – climate relationship is stronger for GPP and RECO than NEE, with increased CO_2 fluxes when 2 m temperature, vapor pressure deficit and evapotranspiration increase and when precipitation and soil moisture decrease. The models forced by dynamic climate conditions clearly outperform those driven by static climate conditions. The "long-term" trend is not obvious for NEE neither in the observations nor in the simulations, partly because both GPP and RECO tend to increase in western Europe. Our results suggest that the spatial resolution of the climate drivers is likely very important for capturing spatial and temporal patterns in CO_2 exchanges and point towards the need to choose the appropriate model and spatial resolution according to the scientific question to deal with.

Key words: Net ecosystem exchange, gross primary production, ecosystem respiration, climate, annual cycle, annual budget, interannual variability, trend

https://doi.org/10.5194/egusphere-2024-1758
Preprint. Discussion started: 20 June 2024

1 Introduction

Among all their environmental benefits, forest ecosystems are efficient carbon sinks and constitute a potential lever for climate change mitigation. At the global scale, forest ecosystems cover about 30% of landmasses. They represent the largest part of the land carbon sink (Lindeskog et al., 2021), with up to 20-50% of anthropogenic CO_2 emissions (land-use changes excluded) sequestered for the 2000-2010 period (Pan et al., 2011; Le Quéré et al., 2018; Pugh et al., 2019). Despite the fertilization effect of increased atmospheric CO_2 concentrations (Walker et al., 2020; IPCC, 2023) and the warming-induced lengthening of the growing season (Prislan et al., 2019; Menzel et al., 2020; IPCC, 2023), the evolution in the net ecosystem exchange (NEE) suggests a recent decrease of annual CO_2 storage in forest ecosystems of temperate Europe, due to severe heat waves and droughts that affected Northern regions in 2018 and Central-Southeastern regions in 2020 (Smith et al., 2020; Thompson et al., 2020; van der Woude et al., 2023). This trend results from a combination of multiple factors. In France, for instance, the CO_2 storage by forests dropped from ~53 Mt CO_2 year^{-1} to ~32Mt CO_2 year^{-1} between 2005-2013 and 2012-2020, mostly due to increased timber-extraction (+20%), climate-related mortality (+54%) and decreased biological production (-10%) (IGN, 2022; Chuine et al., 2023). Such a continental-to-country scale evolution of forest-related CO_2 fluxes needs to be refined at a finer spatial grain to better account for the contributing influence of different forest stands and to clarify the role of forest ecosystems in the CO_2 budget at a territorial level and their leverage in mitigating climate change impacts.

A territorial-scale assessment remains, however, challenging. Measuring NEE and its two components, gross primary production (GPP) quantifying CO_2 sequestration through photosynthesis and ecosystem respiration (RECO) releasing CO_2 through autotrophic and heterotrophic processes, is expensive since it requires the installation and maintenance of flux towers measuring eddy covariance above the canopy (Burba, 2021). The FLUXNET initiative provides over 1500 site-years of quality-controlled flux tower data from 212 sites around the globe, using the same ONEFlux processing pipeline to foster inter-site comparisons (Pastorello, 2020). At the European scale, the Integrated Carbon Observation System (ICOS) network provides standardized and open data from 98 ecosystem stations across 16 countries. The flux towers remain limited in number and unevenly distributed spatially, which makes it impossible to study CO_2 fluxes directly in unequipped sites. Process-based and data-driven models allow us to tackle the above limitation. Process-based models, such as dynamical vegetation models, are routinely used to assess CO_2 flux exchanges between the atmosphere and the biosphere (Friedlingstein et al., 2023). These are mechanistic models (Friedlingstein et al., 2006; Sitch et al., 2008), which allow for testing the response of CO_2 fluxes to individual and combined forcing. Data-driven models rely on the identification of statistical relationships between flux tower measures by eddy-covariance and corresponding land use, vegetation properties and climate characteristics. Based on these statistical relationships, empirical models are built and used for upscaling, i.e., for assessing CO_2 fluxes in regions where they are not measured (Jung et al., 2009, 2019, 2020; Tramontana et al., 2016; Zhuravlev et al., 2022). Both approaches have limitations. For instance, estimations of CO_2 flux exchanges are highly sensitive to physical parameterizations (Cai and Prentice, 2020) and atmospheric forcing (Wu et al., 2017; Hardouin et al., 2022) in process-based models. Regional CO_2 flux upscaling methods are also limited by the sparse and uneven distribution of flux tower measurements, and limitations of the underlying statistical methods used in data-driven models (Jung et al., 2020).

https://doi.org/10.5194/egusphere-2024-1758
Preprint. Discussion started: 20 June 2024

This study aims at comparing the respective strengths and limitations of process-based and data-driven approaches to capture the recent temporal dynamics of CO_2 flux exchanges observed in western European temperate forest ecosystems, with a focus on evergreen needleleaf forests (ENFs) and deciduous broadleaf forests (DBFs). The first objective is to discuss their capability to simulate the mean state, interannual variability and trend in NEE and, when available, GPP and RECO. Previous observation-based studies have shown that CO_2 flux exchanges depend on multiple factors not necessarily related to climate such as soil properties (Kurbatova et al., 2008; Besnard et al., 2018; Curtis and Gough, 2018; Martinez del Castillo et al., 2022), forest management practices (Carrara et al., 2003; Scott et al., 2004; Saunders et al., 2012), tree age (Kurbatova et al., 2008; Besnard et al., 2018; Chuine et al., 2023) and tree species (Carrara et al., 2003, 2004; Welp et al., 2007; von Buttlar et al., 2018; Zheng et al., 2021; Kong et al., 2022) among many others. On average, the annual cycle of CO_2 flux exchanges significantly differs between ENFs and DBFs since photosynthesis can occur all year long in the former, while is bounded from spring (bud break) to fall (leaf senescence) in the latter. As a result, DBFs tend to be a net CO_2 sink during the warm season, and CO_2 source during the cold season (Granier et al., 2002; Welp et al., 2007); whereas, ENFs can persist as a CO_2 sink year-around under favorable meteorological conditions (Mizoguchi et al., 2012). At the interannual timescale, Welp et al. (2007) found that the NEE variability is greater and mainly driven by GPP in Alaskan DBFs and by RECO in the ENFs. This is at odds with Yuan et al. (2009) who found the opposite pattern in 30 northern-hemisphere sites, suggesting latitudinal (hence climate) dependency in the results.

The second study objective is to examine the influence of climate on the temporal variability of CO_2 flux exchanges in temperate DBFs and ENFs in terms of annual cycle (monthly timescale), interannual variability (monthly and annual timescales) and trend (annual timescale). The recent record-breaking temperatures and long drought episodes observed e.g., in Central Europe in 2003, Central and Northern Europe in 2018 and Central and Southeastern Europe in 2022, have been accompanied by sharp reductions in forest CO_2 uptake (Ciais et al., 2005; Thompson et al., 2020; van der Woude et al., 2023). Understanding the role of climate on forest NEE temporal dynamics requires accounting for both monthly and annual budgets since potential compensations of CO_2 fluxes can occur across the annual cycle. This is the case in 2018 in Northern Europe when increased CO_2 uptake in spring (due to anomalously warm conditions) was offset by an anomalous decrease in summer (due to heat and drought), resulting in week NEE anomalies at the annual timescale (Thompson et al., 2020). Understanding the role of climate on NEE also requires assessing how the much larger GPP and RECO component fluxes may respond differently to climate. The annual cycle and, to a lesser extent, the interannual variability of these CO_2 fluxes are driven by temperature and the water cycle, including soil moisture (Haszpra et al., 2005; Tang et al., 2013; Kong et al., 2022; Sharma et al., 2022; Li et al., 2023). Welp et al. (2007) showed that DBFs are more sensitive to soil moisture changes in ENFs than in DBFs, and that decreased GPP under water stress was observed in DBFs only. The authors attributed this difference to a possible buffer effect in ENFs' soils that is damping out temperature increases and to a lower stomatal sensitivity of conifers. In addition, the soil respiration increases exponentially with temperature (van't Hoff, 1898; Meyer et al., 2018) until a maximum temperature threshold is reached, which rarely occurs in extratropical soils (von Buttlar et al., 2018). However, when extreme temperatures are combined with soil water stress, clearer GPP and RECO answers come out. For instance, Ciais et al. (2005) estimated a 30% decrease in GPP and moderate RECO tail-off during the 2003 severe heat and drought event in Central Europe, resulting in a lower net carbon uptake. The larger contribution of GPP on NEE interannual variability remains site and stand dependent (Welp et al., 2007; Yuan et al., 2009). Finally, despite strong effects

https://doi.org/10.5194/egusphere-2024-1758
Preprint. Discussion started: 20 June 2024

of recent heat waves and droughts, the NEE does not always show clear trends in response to recent and projected climate change (Ahlström et al., 2012; Abdalla et al., 2013; Tang et al., 2013; Kong et al., 2022; Martinez del Castillo et al., 2022; Li et al., 2023). One possible hypothesis, tested in our study, is a potential compensation of trends between GPP and RECO.

The novelties of this study rely on (i) the comparison between two data-driven models providing CO_2 flux estimations either globally but at coarse resolution (0.5° x 0.5°) or locally but at the hectometric resolution and (ii) the inclusion of a newly released process-based model constrained by soil moisture satellite data, which provides CO_2 flux estimations for each plant functional type at relatively high space-time resolution (daily; 9 km mesh with 1 km sub-grids). Another originality relies on the multi-scale (annual cycle, interannual variability and trend) assessment of the temporal variability in estimated NEE (and its two components) and its climate drivers.

The paper is structured as follows. Section 2 presents the materials and methods. Section 3 presents our results at the monthly and annual timescales and Sections 4 and 5 discuss the results and give the main conclusions, respectively.

2 Materials & Methods

2.1 Site description

This study focuses on five forest sites: two non-instrumented sites in northeastern France where NEE, GPP and RECO are simulated by process-based and data-driven models, and three sites from the FLUXNET network where NEE is measured and GPP and RECO are calculated (Fig. 1).

The first non-instrumented site is located in the National Park of Forests, a 240,000 ha park mostly covered by DBFs (50%). One DBF plot of 25 ha is selected because soil respiration measures are conducted there by the Biogéosciences laboratory since 2020. This DBF plot, named "Châtillonnais (DBF)" hereafter, is located on a ~380 m plateau and characterized by uneven-aged and mixed DBFs dominated by beech (*Fagus sylvatica)* and oaks (*Quercus robur, Quercus petraea*) with no sylvicultural interventions for ~30 years and by oolitic limestone soils. The second site is located in the Regional Natural Park of Morvan, on the Mont Beuvray, a semi-mountainous domain of 950 ha peaking at 821 m and sitting on volcanic-sedimentary rocks. The Mont Beuvray location is particularly impacted by climate change (Castel et al., 2019), with a mean warming trend reaching 2°C more than the neighboring lowlands over the 1958-2015 period. Two plots are considered for Mont Beuvray: one even-aged large-sized Douglas fir *(Pseudotsuga menziesii)* plots of 15 ha classified as ENF and one even-aged beech plot with continuous cover of 8 ha classified as DBF. These plots are named "Mont Beuvray (DBF)" and "Mont Beuvray (ENF)" hereafter.

https://doi.org/10.5194/egusphere-2024-1758
Preprint. Discussion started: 20 June 2024

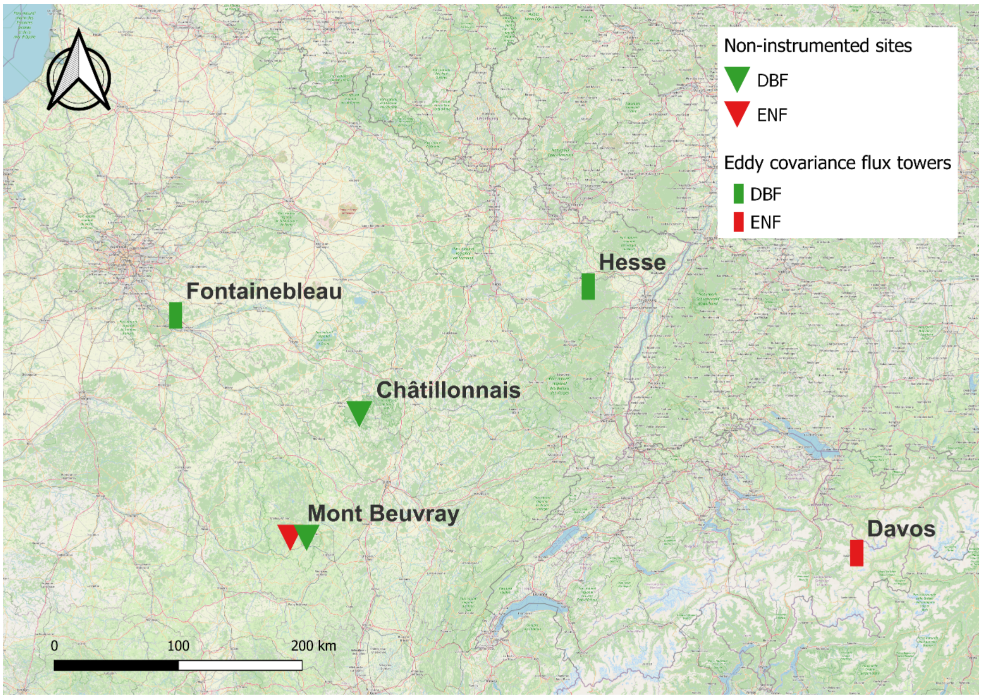

Figure 1: Location of the study sites. The rectangles correspond to FLUXNET sites where CO_2 fluxes are measured by eddy covariance flux towers and estimated by process-based and data-driven models. The triangles correspond to non-instrumented sites where CO_2 fluxes are estimated by process-based and data-driven models only. Symbols in green and red correspond to DBF and ENF sites, respectively. © OpenStreetMap contributors 2021. Distributed under the Open Data Commons Open Database License (ODbL) v1.0.

To compare the CO_2 flux dynamics of these sites and to evaluate the accuracy of data-driven and process-based models, we selected three forest tower sites from the FLUXNET network for their resemblance to the aforementioned ones in terms of location, climate or stand characteristics:

- Two lowland DBFs. The "Fontainebleau" site (FR-Fon) is located in the domanial forest of Barbeau (southeast of Paris), dominated by oak (*Qu. petraea*) and characterized by a loamy soil on top of burstones and deeper marls. The "Hesse" site (FR-Hes) is located in the plain east of the Vosges mountains, dominated by beech (*Fagus sylvatica)* and characterized by a deep silty clay soil on sandstone;
- One midland ENF, "Davos" (CH-Dav), located in the middle range of the subalpine belt in the eastern part of the Swiss Alps at 1639 m, dominated by Norway spruce (*Picea abies)* and characterized by a thin soil on schists and gneiss.

https://doi.org/10.5194/egusphere-2024-1758
Preprint. Discussion started: 20 June 2024

2.2 Carbon flux data

Measured CO_2 fluxes are used as a reference to evaluate outputs from two data-driven and two process-based models (Table 1). They come from the Warm Winter 2020 release (Warm Winter 2020 Team and ICOS Ecosystem Thematic Centre, 2022), an update of the FLUXNET2015 dataset (Pastorello et al., 2020) available on the ICOS platform (https://www.icos-cp.eu/data-products). For each site, we selected daily time series of NEE (NEE_VUT_REF) accounting for multiple friction velocity thresholds and associated with a favorable quality control flag above 80%, GPP (GPP_DT_VUT_REF) and RECO (RECO_DT_VUT_REF). GPP and, to a lesser extent, RECO are less sensitive to the partitioning method (Fig. A1) and the climate – CO_2 flux relationship is similar regardless of the partitioning method used. Here, we retained those CO_2 flux data derived from the daytime flux partitioning method (Lasslop et al., 2010). The temporal coverage of the data is site dependent: 7 years for Hesse, 18 for Fontainebleau and 24 for Davos (Table 1).

	Observations	**Process-based models**		**Data-driven models**	
	FLUXNET	SMAP-L4C	LPJ-GUESS	CarbonSpace	FluxCom
Parameters	NEE, GPP, RECO, weather	NEE, GPP, RECO	NEE, GPP, RECO	NEE	NEE, GPP, RECO
Timescale	Daily	Daily	Hourly	Monthly	Monthly
Spatial resolution	Local	9 km	50 km	Hectometric	50 km
Temporal coverage	Davos: 01/02/1997 – 12/31/2020 Hesse: 01/01/2014 – 12/31/2020 Fontainebleau: 03/11/2005 – 12/31/2022	31/03/2015 – 21/09/2023	01/01/2010 00:00 – 31/12/2022 23:00	01/2000 – 08/2023	01/1979 – 12/2018
Characteristics	Standardized and filtered measurements from flux towers	Carbon model with 1km sub-grids and soil moisture assimilation	Dynamic global vegetation model forced by climate data (ERA5)	Machine learning based estimations, integrating satellite vegetation proxies, climate and flux tower measurements	
References	Pastorello et al. (2020); Warm Winter 2020 Team & ICOS Ecosystem Thematic Centre, 2022)	Jones et al. (2017); Kimball et al. (2022)	Smith et al., (2001, 2014); Wu (2023)	Zhuravlev et al. (2022)	Jung et al. (2019, 2020)

Table 1: Summary of the datasets used in this study.

https://doi.org/10.5194/egusphere-2024-1758
Preprint. Discussion started: 20 June 2024

The two data-driven models use machine learning algorithms for upscaling and make use of observed CO_2 fluxes from the FLUXNET network. The first data-driven model has been developed by the CarbonSpace company. It makes use of (i) a Lagrangian particle dispersion model to account for the footprint of each tower flux site and (ii) a gradient-boosted decision tree based non-linear regression (Chen, 2016) to derive one statistical model per land-cover class. This approach follows that described in Zhuravlev et al. (2022), but with a revised regression methodology and without use of meteorological variables. The Hesse flux tower site is not part of the 84 stations in the FLUXNET2015 dataset used in the model input. A cross-validation is thus possible with Hesse and with measures made after 2015 for the other sites (i.e. 7 years in Davos, 9 years in Fontainebleau). The current model takes the aggregated Köppen–Geiger climate map at 1-km resolution (Beck et al., 2018) as a static predictive variable, but does not yet include temporal climate variability. It provides monthly NEE only but at a very high spatial resolution (few hectares) from 01-2000 to 08-2023. This allows to get as close as possible to the 3 flux tower sites (around 1.8 ha centered on each tower) and their associated CO_2 flux measurement footprints, while also distinguishing each non-instrumented plot (see section 2.1 for details on the area considered).

The second data-driven model comes from the FLUXCOM products (Tramontana et al., 2016; Jung et al., 2019, 2020) retrieved from the data portal of the Max Planck Institute for Biochemistry (https://www.bgc-jena.mpg.de). The FLUXCOM products use eddy-covariance data from 224 flux-tower sites from the FLUXNET La Thuile dataset (http://fluxnet.fluxdata. org/data/la-thuile-dataset/) and the CarboAfrica network (Valentini et al., 2014), including Hesse data between 1997 and 2006 and Fontainebleau between 2005 and 2006. Cross-validations are thus possible with most of our data from the Warm Winter 2020 release. The FLUXCOM products have been shown to accurately estimate the mean annual and seasonal cycles of CO_2 fluxes (Tramontana et al., 2016; Jung et al., 2020; He et al., 2022). Among the various forcing datasets available, we retained three of them, all forced by hourly meteorological data from the ERA5 reanalysis (Hersbach et al., 2020) and providing global maps of monthly NEE, GPP and RECO derived with a daytime partitioning on a 0.5° x 0.5° horizontal grid for the 1979-2018 period. As for FLUXNET, the partitioning method does not significantly affect the CO_2 fluxes (Fig. A2). The three datasets differ according to the algorithm used to build the statistical model: Random Forest (RF; Breiman, 2001), Multivariate Adaptive Regression Splines (MARS; Friedman, 1991) and Artificial Neural Networks (ANNs; Papale and Valentini, 2003). Unlike the CarbonSpace model, their coarse horizontal resolution precludes the ability to account for individual forest stands. Despite these limitations, the three FLUXCOM datasets allow to assess uncertainties induced by the statistical model used for upscaling CO_2 fluxes and to get access to NEE and its two components.

The two process-based models are the Lund-Postdam-Jena General Ecosystem Simulator (LPJ-GUESS; Smith et al., 2001, 2014) and the version 7 of the NASA Soil Moisture Active Passive Mission Level 4 Carbon (SMAP-L4C; Jones et al., 2017; Kimball et al., 2022) models. The LPJ-GUESS is a dynamic global vegetation model simulating the effects of environmental change in vegetation represented by plant functional types (PFTs), soil hydrology and biogeochemistry (Smith et al., 2001). The model is widely used to study ecosystems, including CO_2 fluxes (Smith et al., 2001, 2014; Bayer et al., 2015; Lindeskog et al., 2021; Sathyanadh et al., 2021; Bergkvist et al., 2023). The simulations used here were derived from Wu (2023) using version 4 of LPJ-GUESS in cohort mode forced with hourly ERA5-land reanalysis (Muñoz-Sabater et al., 2021) and observed atmospheric CO_2

https://doi.org/10.5194/egusphere-2024-1758
Preprint. Discussion started: 20 June 2024

concentrations. The cohort mode means that woody plants of the same size and age are represented by a single average individual. Each PFT is represented by multiple average individuals, and one PFT cohort is defined as the average of several individuals. We retrieved hourly NEE, GPP and RECO on a 0.5° x 0.5° horizontal grid for the 2010-2022 period from the ICOS website (https://meta.icos-cp.eu/collections/NZNSUglRn0VeXmGDovuVY0ec). Like the FLUXCOM products, the horizontal resolution of LPJ-GUESS outputs is too coarse to distinguish plots over the Mont Beuvray and Châtillonnais.

The SMAP (Soil Moisture Active Passive) Level 4 Carbon model product (SMAP-L4C) is produced operationally by the NASA SMAP mission and can be considered as a reanalysis product since it uses the Goddard Earth Observing System version 5 (GEOS-5) land model to assimilate SMAP L-band microwave observations and is forced with observed land cover and vegetation from the Moderate Resolution Imaging Spectroradiometer (MODIS) and Visible Infrared Imaging Radiometer Suite (VIIRS). The global processing is conducted on 1 km sub-grids using spatially aggregated MODIS PFTs and VIIRS fPAR inputs, allowing to distinguish up to eight individual PFTs within each 9 km x 9 km product grid cell. However, the model processing uses coarser spatial resolution (9 km and 0.25 degree) daily inputs from the SMAP L4 soil moisture (L4_SM) and GMAO Forward Processor (FP) surface meteorology. Among other variables, the SMAP-L4C outputs provide daily NEE and GPP (RECO deduced from the difference between NEE and GPP), in a consistent global grid from March 2015 to September 2023 for each PFT, including DBFs and ENFs (Jones et al., 2017; Kimball et al., 2022). The 1-km PFT subclass distinction allows to differentiate ENF and DBF behavior over the Mont Beuvray plots. The L4C product is derived using coupled photosynthetic light-use efficiency and soil organic matter decomposition models to estimate daily NEE and it's component carbon fluxes; where, GPP is reduced from PFT-specific optimal rates for unfavorable daily climate conditions including cold temperatures, low light levels, excessive atmospheric vapor pressure deficits and low root zone (0-1m depth) soil moisture levels defined from SMAP L4_SM and GMAO FP meteorology. Details of the model algorithms and the calibration, validation, and performance of the L4C version 7 product used in this study are given in the associated product quality assessment report (Endsley et al., 2023).

2.3 Climate data

Climate parameters are extracted from the version 2 of the operational chain Safran-ISBA-Modcou (SAFRAN-SIM2; Soubeyroux et al., 2008). SAFRAN-SIM2 is an hydrometeorological reanalysis produced by Météo-France at a 8 km spatial resolution from 1958 onwards. For each of the five sites, we extracted the nearest grid point for 2 m temperature (T in °C), soil water index of the first two meters (SWI in %), liquid, solid and total precipitation (PRELIQ, PRENEI and PRE_SUM in mm), real and potential evapotranspiration (EVAP and ETP in mm) and 2 m relative humidity (HU in %). In addition, we calculated the air Vapor Pressure Deficit (in Pa), an integrative metric accounting for both heat and water stress effects (Carrara et al., 2004; von Buttlar et al., 2018; Kong et al., 2022; van der Woude et al., 2023). The VPD is defined as the difference between the amount of moisture that is actually in the air and the amount of moisture that air could hold at saturation. The VPD is computed using the Tetens formula (Monteith and Unsworth, 2007) following Eq. (1):

$$VPD = \left(1 - \frac{HU}{100}\right) * saturation\ vapor\ pressure = \left(1 - \frac{HU}{100}\right)(610.78 * \exp\left(\frac{T}{T+237.3} * 17.2694\right) \qquad (1)$$

https://doi.org/10.5194/egusphere-2024-1758
Preprint. Discussion started: 20 June 2024

Preliminary analyses show that the SAFRAN-SIM2 reanalysis accurately captures the temporal variability and magnitude of 2 m temperature and precipitation compared to observations provided by the three FLUXNET sites (Fig. A3), despite biased solid precipitation in Davos. For this reason and for conciseness, we consider only SAFRAN-SIM2 regardless of the site and CO_2 flux product.

2.4 Methodology

For the gridded datasets (SAFRAN-SIM2, FLUXCOM, LPJ-GUESS and SMAP-L4C), we extracted the nearest grid point to the flux tower sites and to the center of Mont Beuvray and Châtillonnais plots. Since all datasets have different temporal resolution and units (Table 1), they all have been converted to tCO_2 ha^{-1} $month^{-1}$ and aggregated at the monthly timescale. From these monthly values, we computed the mean annual cycle by averaging all years available in each dataset, as well as its interannual variability defined as the standard deviation of monthly values. The annual budget was calculated as the sum of the monthly values, only for complete years (i.e. when no monthly value is missing). Fontainebleau is the only site presenting gaps in the observed time series (in 2005, 2014 and 2017) due to too low-quality control values. The mean annual budget is then computed together with its interannual variability following the same procedure described above.

The model skill in capturing observed CO_2 flux temporal variability at the monthly and annual timescales is assessed over overlapping periods between each model end each observation. Magnitude and co-variability errors are assessed in terms of bias and Bravais-Pearson correlation coefficient (R) or coefficient of determination (R^2), respectively. The evaluation is done considering raw monthly values to focus on the annual cycle, as well as monthly anomalies (i.e., removal of the mean annual cycle) and raw annual values to focus on interannual variability at the monthly and annual timescales, respectively.

The R and R^2 metrics are also used to assess the relationship between climate variables and CO_2 fluxes at the monthly (raw and anomalous values) and annual (raw values) timescales. In addition, a composite approach is performed to examine monthly climate anomalies associated with large negative and positive monthly anomalies in CO_2 fluxes (NEE, GPP and RECO). Large negative/positive CO_2 flux anomalies are defined as standardized anomalies (mean=0, standard deviation=1) below/above -0.5/+0.5. Tests with stricter threshold values (e.g., -1/+1) lead to similar results but limit the size of the samples. The difference between the two groups is tested for significance based on the non-parametric Mann-Whitney *U* test (McKnight and Najab, 2010).

3 Results

3.1 Monthly timescale

3.1.1 Mean annual cycle and interannual variability in climate and CO_2 fluxes

https://doi.org/10.5194/egusphere-2024-1758
Preprint. Discussion started: 20 June 2024

Figure 2 shows the mean annual cycle and interannual variability of T and main surface water cycle parameters associated with each site. All sites follow similar patterns of T, ETP, EVAP and VPD with the greatest values in summer and the lowest in winter. The annual cycle in SWI is reversed, with drier soils in late summer and wetter soils in winter. The total precipitation is evenly distributed throughout the year for sites in plain (Fontainebleau and Hesse and Châtillonnais), in contrast with mountainous sites (Davos and Mont Beuvray) where precipitation amounts are larger during winter than summer. The interannual variability (shadings on Fig. 2) is particularly pronounced all year long for PRE_SUM and from spring to fall for VPD, highlighting strong year-to-year fluctuations of the water cycle.

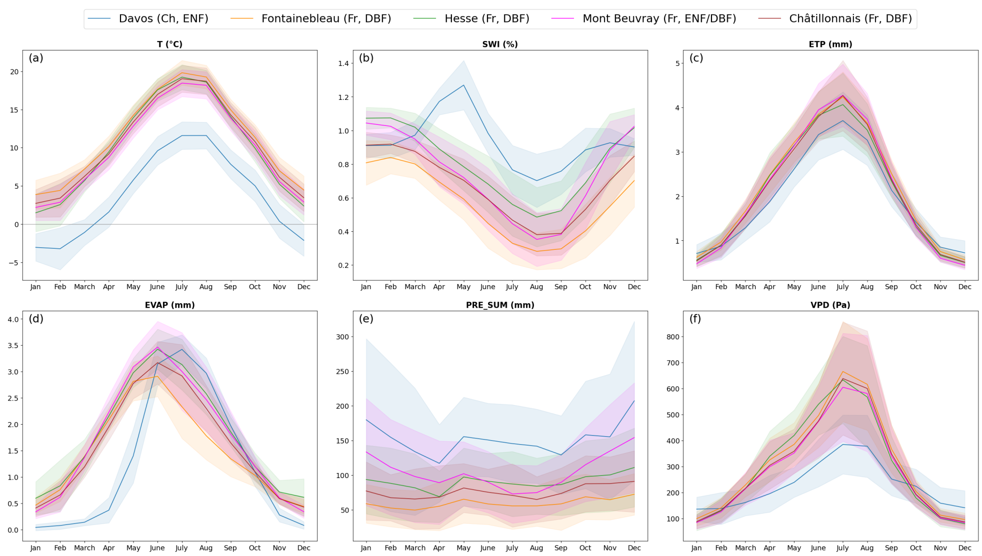

Figure 2: Mean annual cycle and interannual variability in monthly (a) 2 m air temperature (T), (b) soil moisture of the first two meters (SWI), (c) potential evapotranspiration (ETP), (d) real evapotranspiration (ETR), (e) total precipitation (liquid + solid: PRE_SUM) and (f) vapor pressure deficit (VPD) for each study site (colors, see insert) for the 1990–2023 period. Climate conditions in each site are extracted from the nearest grid point of the 8 km x 8 km SAFRAN-SIM2 reanalysis. Bold lines show the mean annual cycle. Shadings show interannual variability computed as the standard deviation of each month of the period.

Due to its much higher elevation, Davos depicts different climate conditions than the other sites with (i) lower T by up to ~10 °C all year long, (ii) wetter soils, especially in spring due to mild temperature, low evaporation and snow melting (not shown), (iii) larger precipitation amounts all year long with snowfall from October to April (not shown) and (iv) delayed EVAP peak in late summer. While this site is not an analogue of the Mont Beuvray ENF site, it remains the most representative one available in the FLUXNET network.

The mean annual cycle of monthly NEE is marked in all study sites (Fig. 3). Temperate forest ecosystems release CO_2 during winter and sequester CO_2 during summer, with higher values in summer than in winter. While this overall cycle prevails all years, the sign of the NEE can be reversed from one year to another in spring and fall in

https://doi.org/10.5194/egusphere-2024-1758
Preprint. Discussion started: 20 June 2024

almost all products and sites, indicating that during these seasons the forest ecosystems can be either a CO_2 source or a CO_2 sink. Seasonal contrasts are stronger in DBF than ENF sites, consistent with the DBF leafing seasonality and with previous studies hypothesizing a buffer effect in ENF soils (e.g., Welp et al., 2007; Zheng et al., 2021). The magnitude of interannual variability seems also to be influenced by forest stand characteristics (e.g., in Mont Beuvray in the SMAP-L4C and CarbonSpace models), with e.g. a variability 40% higher for DBFs than ENFs simulated by the CarbonSpace model in Mont Beuvray in July. Despite high coupling between GPP and RECO, the NEE mean annual cycle is mostly driven by GPP in summer and by RECO in winter regardless of the sites, as illustrated for one DBF site in Fig. 4.

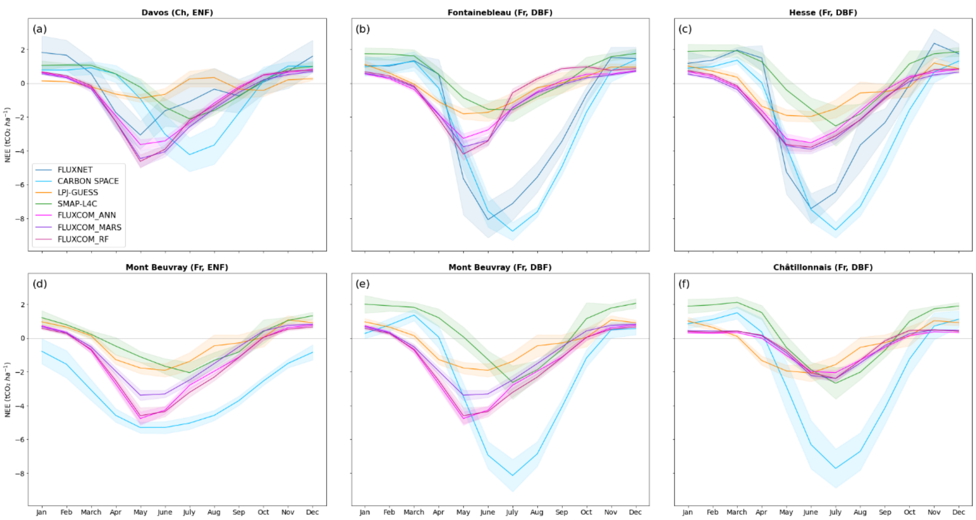

Figure 3: Same as Fig. 2 but for monthly NEE in the (a-c) three FLUXNET sites and (d-f) three non-instrumented sites located in Burgundy as measured by eddy-covariance (FLUXNET) and simulated by data-driven (CarbonSpace and FLUXCOM) and process-based (LPJ-GUESS and SMAP-L4C) models. The longest available period for each site and dataset is retained. See Table 1 for details. For LPJ-GUESS, SMAP-L4C and FLUXCOM models, the nearest grid point from each site is shown. Results from LPJ-GUESS and FLUXCOM are similar in panels (d-e) due to coarse horizontal resolution (0.5° x 0.5°) and no distinction between forest stands (DBF or ENF).

https://doi.org/10.5194/egusphere-2024-1758
Preprint. Discussion started: 20 June 2024

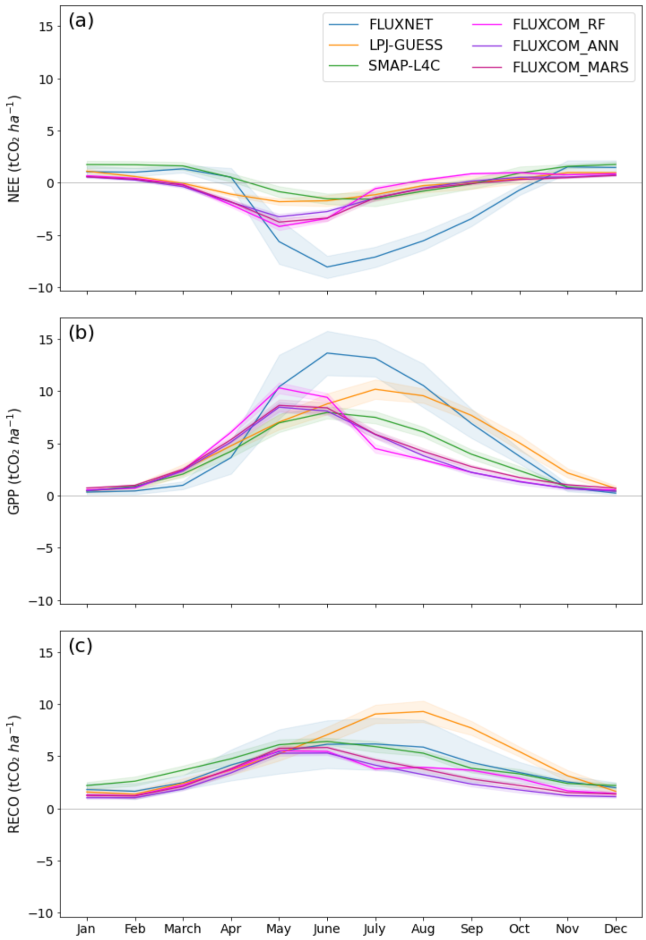

Figure 4: Same as Fig. 3 but for monthly (a) NEE, (b) GPP and (c) RECO in the Fontainebleau DBF site according to FLUXNET observations, FLUXCOM data-driven and LPJ-GUESS and SMAP-L4C process-based models. The CarbonSpace model is not shown since GPP and RECO are not available for this model.

The model skill in capturing monthly NEE depends on the metrics, sites and products (Fig. 5). Overall, the annual cycle in NEE is better represented in the two DBF sites, located in the plain, than the ENF site, Davos, located in the Alps Mountain area (Fig. 5a-c). The reverse holds in terms of magnitude (Fig. 5d-f). In Davos, all models reasonably capture the magnitude of monthly NEE, with inter-quartile in the -2 and +2 $tCO_2\ ha^{-1}$ range, while the FLUXCOMs are the only models to reasonably capture the NEE annual cycle (R^2 inter-quartile in the 0.6-0.7 range). In the two DBF sites, the CarbonSpace data-driven model clearly provides the best scores for both metrics (R^2 in the 0.8-0.9 range and bias in the 0 – -2 $tCO_2\ ha^{-1}$ range), suggesting an added value of very high spatial resolution upscaling for representing CO_2 flux annual cycle and magnitude. The remaining models strongly underestimate the CO_2 uptake during summer and CO_2 release during winter, with 25% of the NEE values

https://doi.org/10.5194/egusphere-2024-1758
Preprint. Discussion started: 20 June 2024

associated with biases exceeding 3-4 tCO_2 ha^{-1} in both DBF sites. Interestingly, the model deficiencies in capturing (i) the annual cycle in NEE is mainly linked to poorly resolved temporal variability of RECO (Fig. A4) and (ii) the biased NEE magnitude is mainly linked to underestimated CO_2 uptake by photosynthesis (Fig. A5).

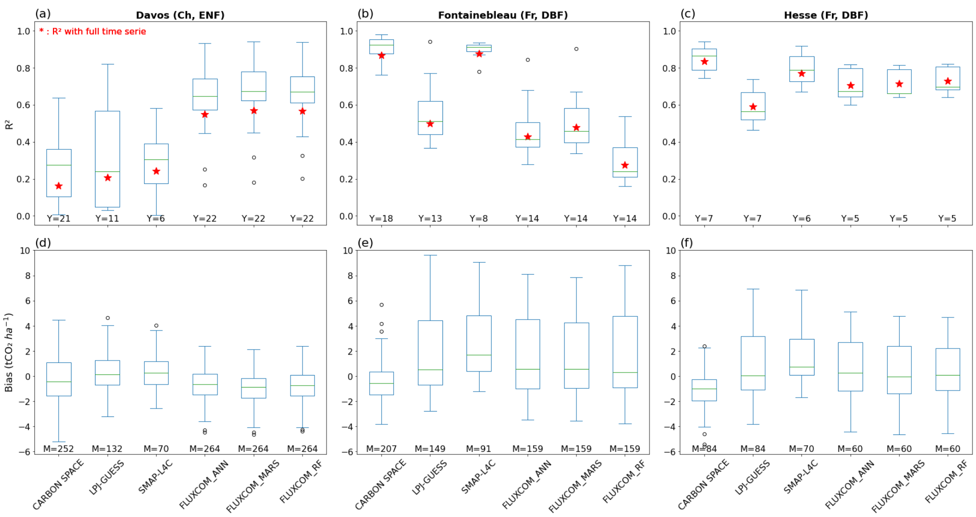

Figure 5: Skill of data-driven and process-based models in capturing the (a-c) annual cycle and (d-f) magnitude in monthly NEE for each FLUXNET site. (a-c) The quality of the annual cycle is assessed through the coefficient of determination (R^2) between simulated and observed monthly NEE (12 values) computed for each overlapping year (labeled on panels a-c). (d-f) The magnitude errors are computed as the difference (i.e., bias) between simulated and observed NEE for each month of the overlapping period (labeled on panels d-f). The boxes have lines at the lower quartile, median, and upper quartile values. The whiskers are lines extending from each end of the boxes to show the extent of the range of the data within 1.5 by inter-quartile range from the upper and lower quartiles. Circles are outliers and red crosses in panels (a-c) are R^2 computed considering the full monthly timeseries at once (e.g., 252 months for the first from left boxplot in panel a).

The annual cycle and magnitude of NEE simulated in the ENF and the two DBF non-instrumented plots (Fig. 3d-f) closely resemble those simulated in the instrumented sites (Fig. 3a-c). The two main exceptions concern all-year-long CO_2 sequestration simulated by the CarbonSpace model in the Mont Beuvray ENF site, and much weaker CO_2 sequestration peak simulated by the FLUXCOM models in the Châtillonnais DBF site. Based on these results, the CarbonSpace data-driven model appears to be the best compromise to capture the annual cycle and magnitude of NEE associated with both ENFs and DBFs. The results also demonstrate that process-based and data-driven models have their own strengths and weaknesses and are thus complementary.

3.1.2 Climate – CO_2 flux relationship

The CO_2 flux – climate relationship is assessed considering both raw monthly values to account for the annual cycle and monthly anomalies (i.e., mean annual cycle removed) to focus on interannual variability.

https://doi.org/10.5194/egusphere-2024-1758
Preprint. Discussion started: 20 June 2024

The synchronous relationship between the annual cycle of CO_2 fluxes and that of various climate parameters is assessed through a correlation analysis of raw monthly time series (Fig. 6). Regardless of the sites and models, T, VPD, ETP and EVAP correlate the most with NEE. For these parameters, the correlation coefficients are negative meaning that CO_2 uptake increases with higher T, VPD and evapotranspiration. The weakest correlations are found for PRE_SUM and, to a lesser extent, SWI. Although we can hypothesize that climate variables are interdependent, a variance inflation factor (VIF) calculation highlighted the existence of multicollinearity only between ETP and VPD (VIF>5 in almost all sites and models).

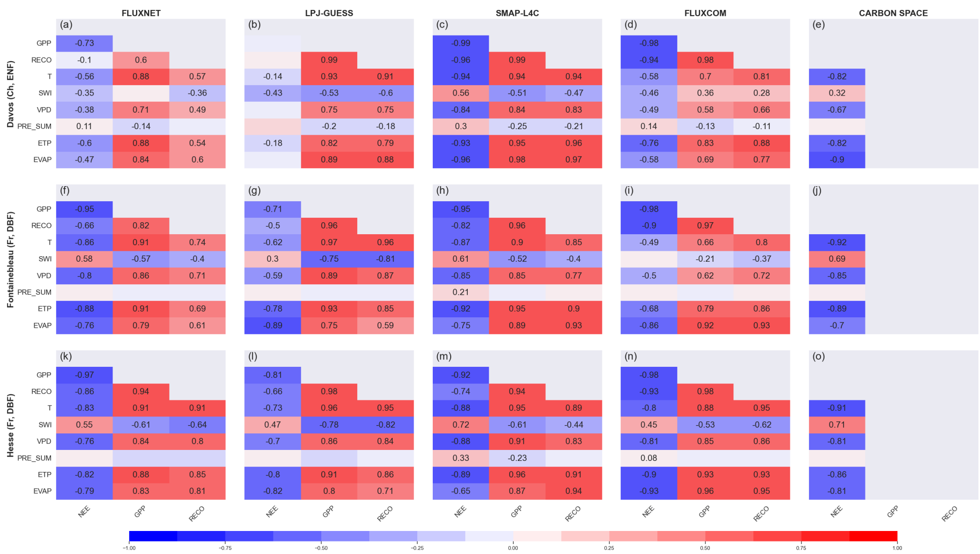

Figure 6: Bravais Pearson correlation coefficient values (shadings) between the three CO_2 flux variables from each model and site, and the associated SAFRAN-SIM2 climate parameters associated with each site location. Climate parameters include 2 m air temperature (T in °C), soil water index (SWI in %), vapor pressure deficit (VPD in Pa), total precipitation (PRE_SUM in mm), potential and real evapotranspiration (ETP and EVAP in mm). (a-e) Davos, (f-j) Fontainebleau and (k-o) Hesse FLUXNET sites. Correlations are computed considering all months and all years for overlapping periods between climate and CO_2 flux datasets. See Table 1 for details. The FLUXCOM multi-model mean is shown in panels d,i,n for conciseness since the three FLUXCOM models provide similar results. GPP and RECO are not shown in panels e,j,o because they are not provided by the CarbonSpace data-driven model. Only correlation values significant at the 90% confidence level are written.

Three main results emerge when comparing the influence of climate on the annual cycle in NEE, GPP and RECO. First, the climate influence is most of the time greater on GPP than RECO, particularly in the FLUXNET observations, meaning that photosynthesis is more affected by climate conditions than are respiration processes. Second, the climate influence can be strong on both GPP and RECO but weak on NEE (Fig. 6). This is for instance the case in Davos where the correlation coefficient between T and LPJ-GUESS-simulated CO_2 fluxes exceeds 0.9 for both GPP and RECO while remains weak and barely significant for NEE. Last, the climate influence on the

https://doi.org/10.5194/egusphere-2024-1758
Preprint. Discussion started: 20 June 2024

annual cycle in simulated CO_2 fluxes highly depends on the model capability to capture the CO_2 flux annual cycle. From this point of view, the CarbonSpace data-driven and SMAP-L4C process-based models often depict stronger CO_2 fluxes – climate relationships than the remaining models, consistent with more accurate simulation of the CO_2 flux annual cycle (Fig. 3).

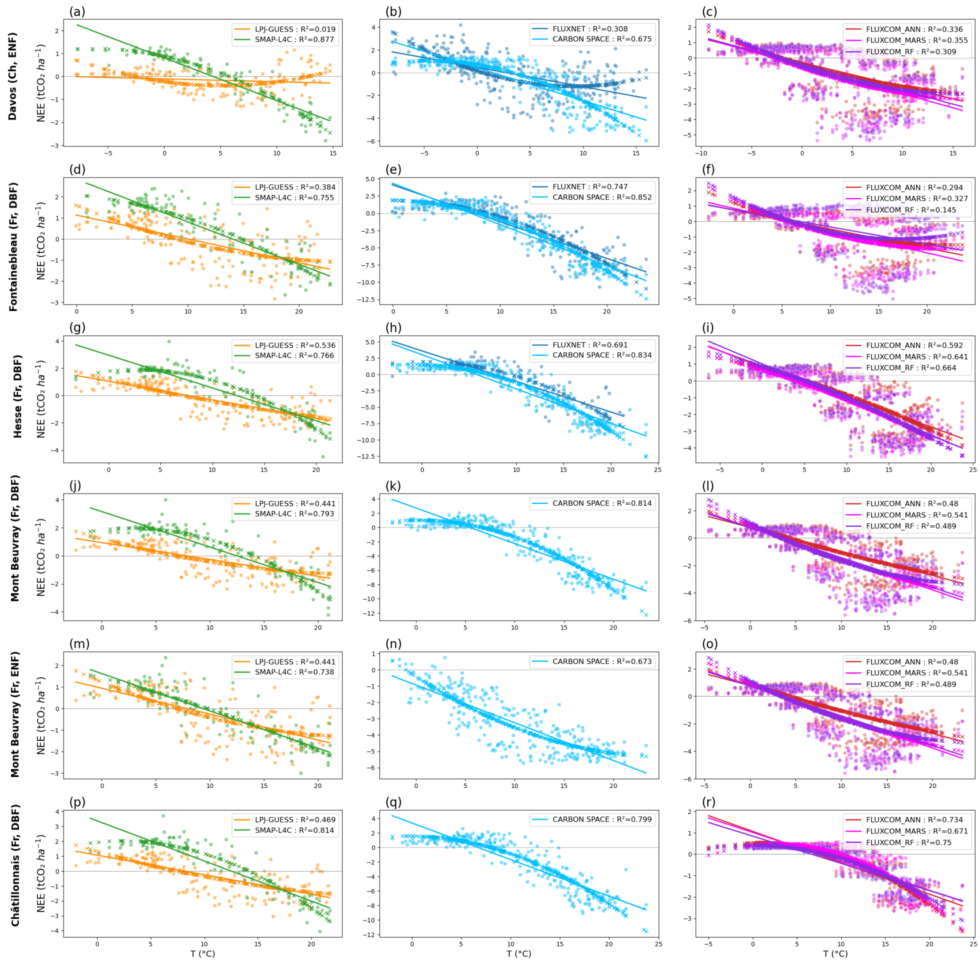

Figure 7: Simple linear and 2nd order polynomial regressions between monthly 2 m temperature from SAFRAN-SIM2 (x-axis) and NEE (y-axis) from all datasets and sites. (a,d,g,j,m,p) LPJ-GUESS and SMAP-L4C process-based models. (b,e,h,k,n,q) FLUXNET observations and CarbonSpace data-driven model. (c,f,i,l,o,r) FLUXCOM data-driven models. The coefficient of determination (R^2) in the insert is derived from the linear regression.

A particular attention is given on the relationship between T and NEE (Fig. 7) to further discuss uncertainties induced by the products and dependencies to forest stand conditions. The relationship is systematically weaker (i) in Davos than in other sites regardless of the product and (ii) in the two coarse resolution models (LPJ-GUESS and FLUXCOM) regardless of the site. The relationship is linear-like in ENF sites regardless of the dataset and

https://doi.org/10.5194/egusphere-2024-1758
Preprint. Discussion started: 20 June 2024

the CO_2 flux. This contrasts with DBF sites where the observed T – NEE relationship is polynomial with an evident threshold effect. Below 10°C, the NEE turns positive, indicating a net ecosystem carbon loss, and stabilizes in the 0–2 $tCO_2\ ha^{-1}$ range. This threshold effect corresponds to the low biological activity of DBFs under cold conditions, hence weak to no CO_2 uptake by photosynthesis. This threshold effect results thus from GPP only, as reflected by the flattening of the GPP curve at low T (Fig. A6) unlike the linear RECO – T relationship (Fig. A7). Among the models, the SMAP-L4C and CarbonSpace are the only models to capture the observed threshold, highlighting the usefulness of distinguishing the PFT in the model outputs.

The above analyses (Figs. 6-7) depict significant relationships between climate and CO_2 fluxes when accounting for the annual cycle. Once the latter is removed (see section 1.4 for details), most of the correlation values are higher for process-based than data-driven models, remain of the same sign but are of weaker magnitude for GPP and RECO and are almost negligible for NEE (Fig. 8). Positive anomalies in GPP and RECO are associated with positive anomalies in T, VPD and ETP and negative anomalies in soil moisture (SWI) and, to a lesser extent, precipitation in most sites and products. The reverse holds true for negative GPP and RECO anomalies. The similar response of GPP and RECO to the climate anomalies induces a compensation effect on the residual NEE carbon flux, resulting in weak NEE anomalies. The sign of NEE anomalies is uncertain among the sites and the products and depends on which of the two components is associated with the largest anomalies. While the models tend to exaggerate the observed relationship between CO_2 flux and climate anomalies, especially the process-based models, the overall picture is satisfactorily captured.

Figure 8: Same as Fig. 6 but after removing the mean annual cycle.

In addition to the correlation analysis, for which few disagreements can lead to poor correlation values, we now investigate climate anomalies associated with the largest anomalies in monthly CO_2 fluxes (see Section 2.4 for

https://doi.org/10.5194/egusphere-2024-1758
Preprint. Discussion started: 20 June 2024

details). Results are shown for the Fontainebleau DBF site only for conciseness in Figs. 9-11. The main results can be summarized as follows. Two main climate parameters, PRE_SUM and T, appear to significantly influence the largest CO_2 flux monthly anomalies in almost all datasets. Wet anomalies significantly favor anomalies that are positive for RECO and negative for GPP, hence less CO_2 uptake (Figs. 9c, 10c and 11c), and vice versa for dry anomalies. Warm anomalies are associated with large positive NEE anomalies (i.e., strong CO_2 emissions or weak CO_2 uptake) and vice versa for cold anomalies (Fig. 9a). In turn, the DBF ecosystem sequesters less (more) CO_2 during anomalously warm (cold) conditions. This result is more clearly driven by RECO (Fig. 10a) than GPP (Fig. 11a), consistent with an exponential response of respiration to T (van't Hoff, 1898). Some relationships are opposite in sign between the process-based models and the data-driven models, highlighting strong uncertainties induced by the approach. For instance, anomalously dry soil is associated with RECO and GPP anomalies that are positive in the process-based models, especially LPJ-GUESS, while negative in the FLUXCOM data-driven models (Figs. 10b and 11b).

https://doi.org/10.5194/egusphere-2024-1758
Preprint. Discussion started: 20 June 2024

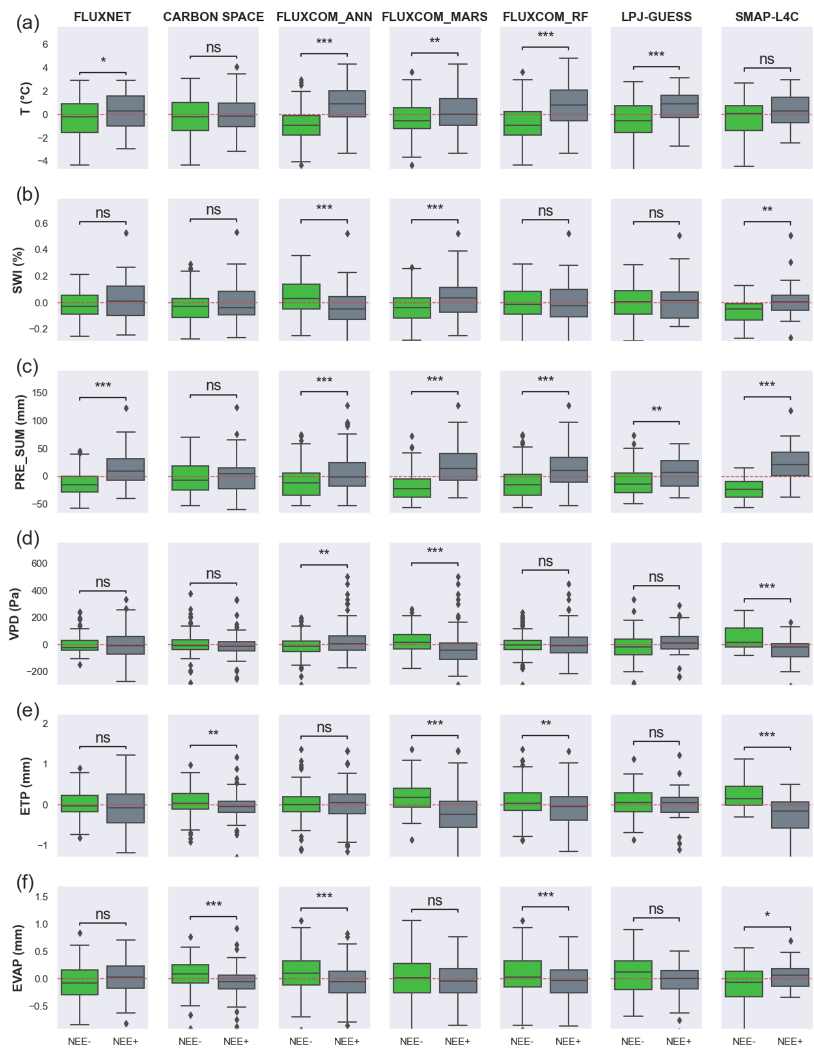

Figure 9: Monthly climate anomalies associated with large negative and positive anomalies in monthly NEE (NEE- and NEE+, respectively) for each dataset in the Fontainebleau DBF site. (a) 2m temperature (°C). (b) Soil water index (%). (c) Total precipitation (mm/month). (d) Vapor pressure deficit (Pa). (e) Potential evapotranspiration (mm/month). (f) Real evapotranspiration (mm/month). NEE- (NEE+) anomalies are defined as standardized anomalies (mean=0; standard deviation=1) below -0.5 (above 0.5). The boxes have lines at the lower quartile, median, and upper quartile values. The whiskers are lines extending from each end of the boxes to show the extent of the range of the data within 1.5 by inter-quartile range from the upper and lower quartiles. Circles are outliers. The symbol ns indicates no statistically significant difference in climate anomalies between NEE- and NEE+ according to a Mann-Whitney *U* test. The symbols *, ** and *** correspond to significant differences at the 90, 95 and 99% confidence level according to the same test.

https://doi.org/10.5194/egusphere-2024-1758
Preprint. Discussion started: 20 June 2024

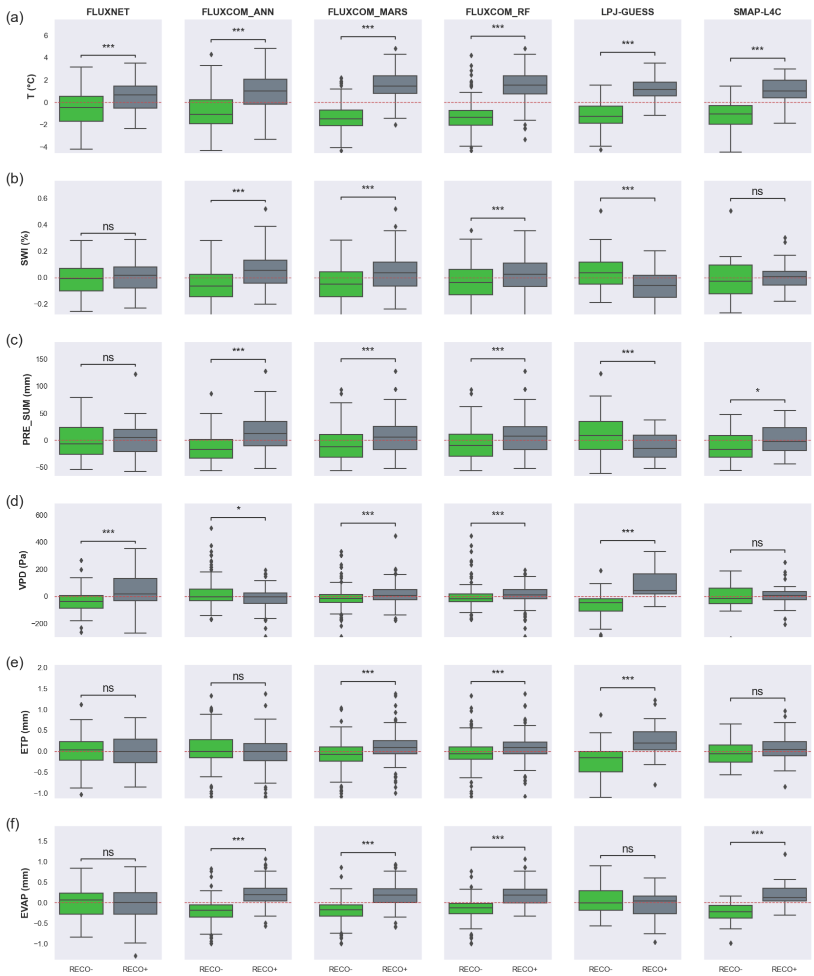

Figure 10: Same as Fig. 9 but for RECO.

https://doi.org/10.5194/egusphere-2024-1758
Preprint. Discussion started: 20 June 2024

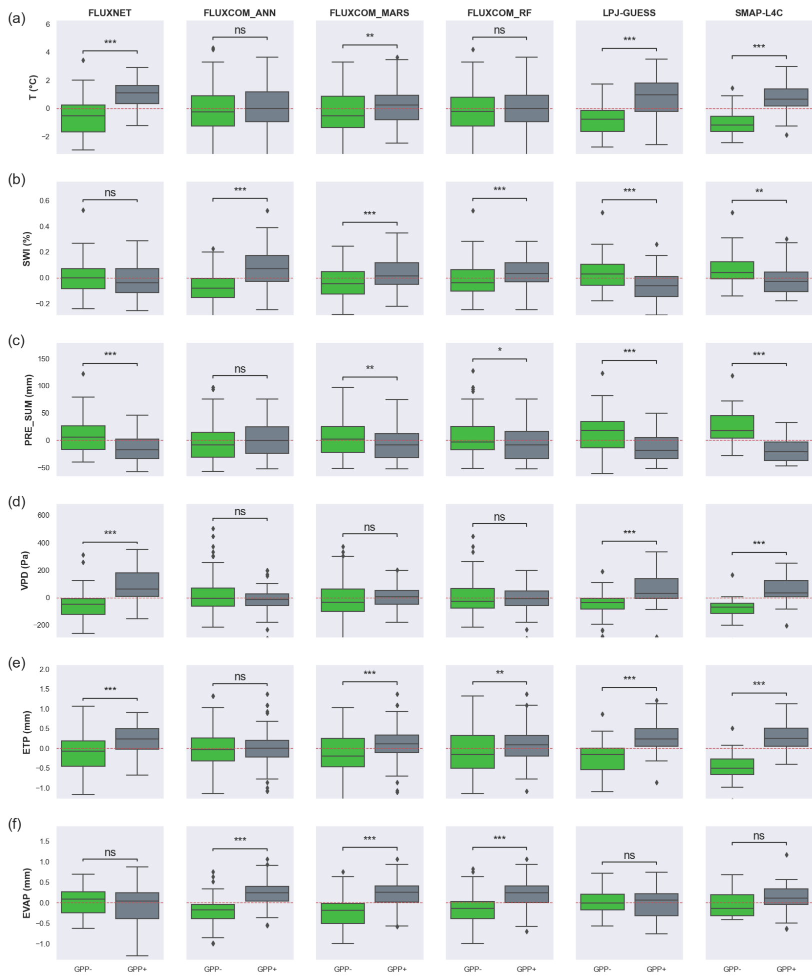

Figure 11: Same as Fig. 9 but for GPP.

This section demonstrates that the annual cycle of monthly CO_2 fluxes is sharply driven by climate, while its interannual variability is not a simple response to climate anomalies. Most of the models accurately capture the observed annual cycle and its relationship with climate. However, the interannual variability of monthly CO_2 flux anomalies are not necessarily phased between observations and models (i.e., weak co-variability), especially for NEE, and the models tend to exaggerate the impact of climate on CO_2 flux interannual variability.

https://doi.org/10.5194/egusphere-2024-1758
Preprint. Discussion started: 20 June 2024

3.2 Annual timescale

3.2.1 Mean annual budget and interannual variability

In the observations, the mean annual CO_2 sequestration of the ecosystems is, on average, far weaker in the ENF site (-2.24 tCO_2 ha^{-1} $year^{-1}$) than the DBF sites (-24.63 tCO_2 ha^{-1} $year^{-1}$ in Fontainebleau and -15.14 tCO_2 ha^{-1} $year^{-1}$ in Hesse), while the reverse holds in terms of interannual variability (±6.92 against 3.92 and 3.60 tCO_2 ha^{-1} $year^{-1}$, respectively) (Fig. 12a). The large contrast between DBF and ENF sites may not be transposable since climate in Davos is atypical, with much colder and wetter mean conditions and larger year-to-year variability compared to the remaining sites (Fig. 2). Only the two process-based models (LPJ-GUESS and SMAP-L4C) provide mean annual CO_2 uptake values comparable to observations in Davos. However, this might be a coincidence since these models strongly underestimate the NEE annual budget in the other sites due to underestimated GPP (Fig. 12b) and overestimated RECO (Fig. 12c). In particular, the NEE annual budget is positive in all DBF sites in the SMAP-L4C owing to a too short duration of the uptake season simulated by this model (Fig. 3), resulting in annual GPP bias of e.g. -21.77 tCO_2 ha^{-1} $year^{-1}$ in Fontainebleau (Fig. 12b).

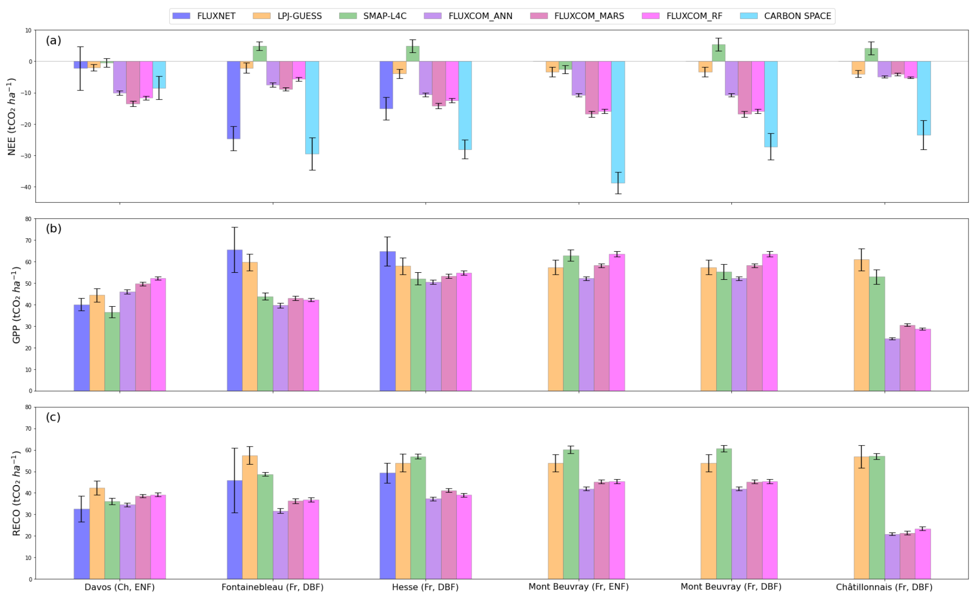

Figure 12: Mean annual budget (bars) and interannual variability (whiskers) in (a) NEE, (b) GPP and (c) RECO for each site and dataset. Note that the results are similar in the Mont Beuvray ENF and DBF sites for the LPJ-GUESS and FLUXCOM models due to their coarse resolution and no distinction of the forest stand in the outputs.

Except in Davos, the two data-driven models perform reasonably well to capture the observed magnitude of NEE annual budget, despite CO_2 uptake in DBF sites is underestimated by 15 to 20 tCO_2 ha^{-1} $year^{-1}$ in Fontainebleau by the FLUXCOM models and overestimated by 19.99 tCO_2 ha^{-1} $year^{-1}$ in Hesse by the CarbonSpace model. Over Mont Beuvray, the annual CO_2 uptake is greater in the ENF than the DBF site for the models distinguishing the

https://doi.org/10.5194/egusphere-2024-1758
Preprint. Discussion started: 20 June 2024

PFTs in their outputs (i.e., CarbonSpace and SMAP-L4C). This might be explained by a basal area reaching 49 m^2 ha^{-1} in average in the ENF plot against 32 m^2 ha^{-1} in the DBF one (for a volume of 656 m^3 ha^{-1} and 404 m^3 ha^{-1}; data based on forest inventory), inducing a weaker photosynthetic activity in the DBF (Fig. 12b). This hierarchy cannot be captured by the FLUXCOM and LPJ-GUESS models by construction since the two Mont Beuvray plots are part of the same grid point and ENF and DBF are not distinguished.

At the interannual timescale, the forest ecosystem systematically acts as a CO_2 sink (Fig. 12), except (i) in Davos for the observations and the SMAP-L4C model and (ii) in all DBF sites for the SMAP-L4C model where NEE is always positive (i.e., CO_2 release), as already discussed. The magnitude of interannual variability in annual NEE is the largest and the closest to the observed one for the CarbonSpace model (±3.92 and 5.16 tCO_2 ha^{-1} $year^{-1}$ in Fontainebleau), and the lowest and farthest from the observed one for the FLUXCOM models (±0.55 tCO_2 ha^{-1} $year^{-1}$ in Fontainebleau with FLUXCOM_MARS), a statement also prevailing for GPP and RECO.

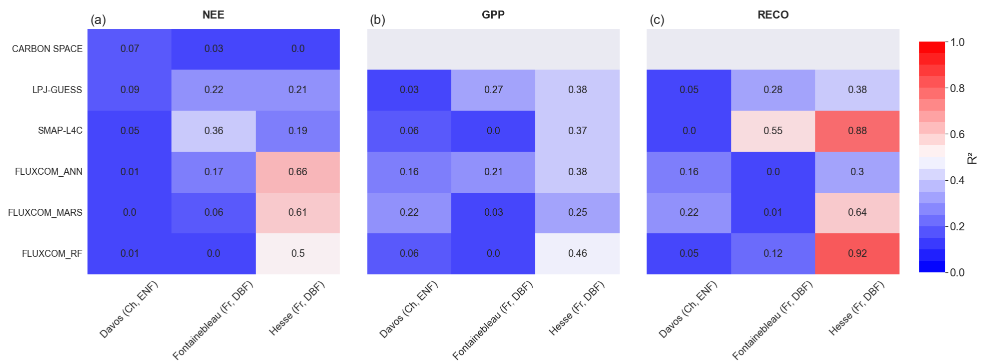

Figure 13: Coefficient of determination (numbers and shadings) between modelled and measured fluxes in the FLUXNET sites at the annual timescale.

Beyond the magnitude of interannual variability, a critical question concerns the model capability to capture the observed year-to-year fluctuations of annual CO_2 fluxes (Fig. 13). No model succeeds at capturing the observed NEE, GPP and RECO interannual variability in Davos, suggesting deficiencies of state-of-the-art models in simulating CO_2 flux interannual variability in mountainous regions. At least for SMAP-L4C, this may be due to the inability of the coarse (0.25 degree resolution) GEOS FP daily meteorology and (9-km grid) SMAP L4 soil moisture to capture the larger spatial heterogeneity in local climate conditions imposed from the complex mountain terrain at this site. For the remaining sites, the models tend to better perform with GPP and RECO than NEE. The CarbonSpace model fails at capturing the observed interannual variability in annual NEE ($R^2 \leq 0.08$). Despite biased annual mean conditions (Fig. 12), the SMAP-L4C performs reasonably well, with R^2 of 0.36 and 0.55 for NEE and RECO in Fontainebleau and 0.88 for RECO in Hesse (Fig. 13). This model is the only one to be forced by satellite observation informed soil moisture, suggesting this parameter is valuable for simulating realistic year-to-year fluctuations of annual CO_2 fluxes. The FLUXCOM models also capture correctly the interannual variability in Hesse for all CO_2 fluxes and perform better (with still low R^2) in Davos for GPP and RECO than the other

https://doi.org/10.5194/egusphere-2024-1758
Preprint. Discussion started: 20 June 2024

models. Importantly, this skill is not "forced" by construction since the Davos site is not used to train the FLUXCOM models, and there is no or few (2) overlapping years between the period used to train the models and that analyzed in our study for Hesse and Fontainebleau. The LPJ-GUESS provides intermediate scores, with R^2 in the 0.3 – 0.4 range. These results indicate that (i) models accounting for climate variability better capture interannual variability in CO_2 fluxes and (ii) the simulated interannual variability is closer to observations at the annual than monthly timescale.

3.2.2 Relationship with climate

Overall, the interannual co-variability between CO_2 flux and climate is qualitatively similar at the annual (Fig. 14) than the monthly (Fig. 8) timescale, with correlation values of the same sign. The main difference concerns less significant correlation values at the annual than monthly timescale for most variables, probably due to a sample size effect since the number of years under study is limited. The only exception concerns a stronger precipitation – CO_2 flux relationship at the annual than monthly timescale for the two process-based models, especially for GPP and RECO with decreased CO_2 fluxes during wet years.

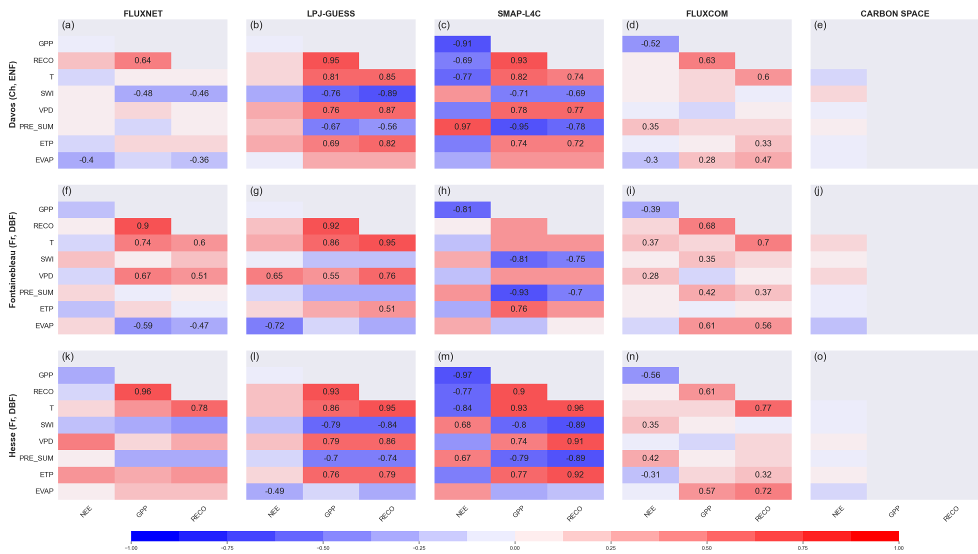

Figure 14: Same as Fig. 6 but for raw annual values.

The "long-term" evolution in the NEE annual budget does not depict any trend but is characterized by strong year-to-year fluctuations, except for the FLUXCOM models depicting surprisingly flat variability (Fig. 15). A modest increase is looming in the very last years of FLUXNET data, especially in DBF plots (Fig. 15b-c) but, as for all other models, the temporal coverage seems too short and the interannual variability too strong to settle any conclusion. Our result contrasts with recent literature pointing towards reduced CO_2 uptake in Europe (Smith et al., 2020; Thompson et al., 2020; Chuine et al., 2023; van der Woude et al., 2023). Possible reasons involve the

https://doi.org/10.5194/egusphere-2024-1758
Preprint. Discussion started: 20 June 2024

limited number of sites under study, the fact that eddy-covariance flux tower measurements may be located in healthy forest ecosystems and potential compensation effects between GPP trends and RECO trends. The latter point is critical, at least in the FLUXNET observations and LPJ-GUESS simulations (Figs. A8-A9). To further test this hypothesis, Figure 16 shows the temporal evolution of annual anomalies in observed CO_2 fluxes and climate parameters in the Fontainebleau DBF site. While annual NEE anomalies do not depict any trend (Fig. 16a), GPP and RECO anomalies are most frequently negative before 2014 and positive afterwards (Fig. 16b). The time series is too short to conclude whether such an evolution is reminiscent of a trend or a decadal-like variability. However, this pattern is consistent with the evolution of annual climate anomalies depicting drier conditions, larger potential evapotranspiration and colder temperature before 2014 than afterwards (Fig. 16c-e).

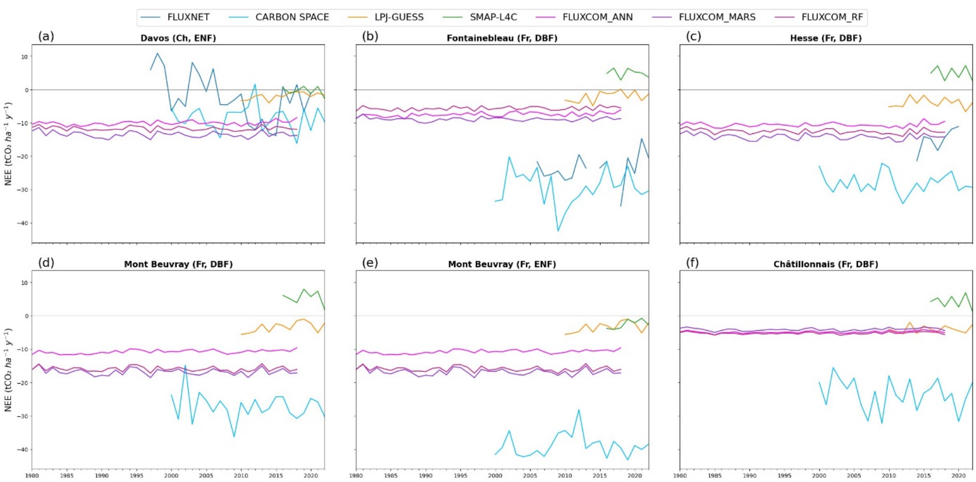

Figure 15: Annual NEE for the longest available period for each site and dataset. Gaps are due to not complete years (e.g. FLUXNET data in Fontainebleau in panel b).

https://doi.org/10.5194/egusphere-2024-1758
Preprint. Discussion started: 20 June 2024

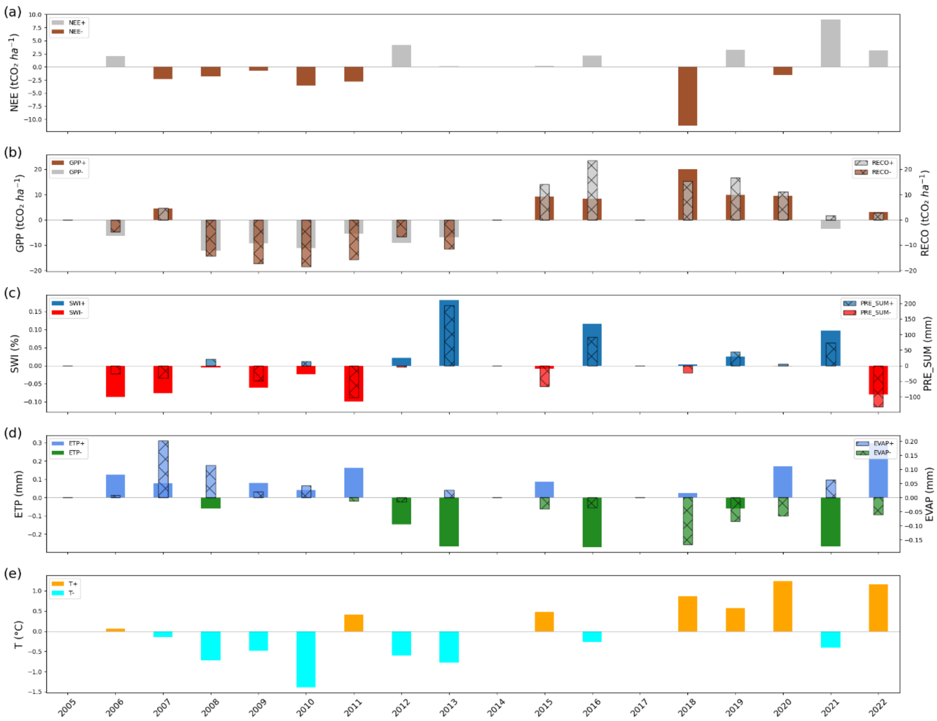

Figure 16: Evolution of annual anomalies in observed CO_2 budget and SAFRAN-SIM2 climate in Fontainebleau between 2005 and 2022. (a) NEE. (b) GPP and RECO. (c) Soil moisture and total precipitation. (d) Real and potential evapotranspiration. (e) 2 m temperature. Anomalies are computed as the difference between each year and the 2005-2022 averaged conditions. The years 2005, 2014 and 2017 have not been accounted for because of missing CO_2 flux data.

4 Discussion

This study aims at evaluating process-based and data-driven models in capturing CO_2 flux temporal dynamics of temperate forest ecosystems and their relationships with climate. Such an evaluation is required to question the extent to which these models may provide relevant information for monitoring CO_2 temporal dynamics and understanding their drivers in temperate forests where no CO_2 measure is available.

First, we show that the model skill depends on the target. On the one hand, the magnitude and pattern of the annual cycle, annual budget and the range of interannual variability (i.e., standard deviation of monthly or annual values) are better captured by the CarbonSpace data-driven model than the remaining models. This added value was expected in e.g. Fontainebleau, since this site is included in the pool of flux tower measurements used for the model calibration, but not in Hesse since this site is not included. Furthermore, the CarbonSpace clearly outperforms the other data-driven models tested (FLUXCOM models set with different AI algorithms), which are

https://doi.org/10.5194/egusphere-2024-1758
Preprint. Discussion started: 20 June 2024

also calibrated with flux tower measurements. This suggests that the accurate skill of the CarbonSpace model relies also on the inclusion of high resolution multi-spectral satellite data allowing to assess CO_2 dynamics at the hectometric scale and to distinguish different PFTs. On the other hand, the co-variability between observations and models, and between CO_2 fluxes and climate depends on whether the focus is on the annual cycle or on the interannual variability. When focusing on the annual cycle (Figs. 4-7), the co-variability is the largest for models capturing the observed annual cycle in CO_2 fluxes, with CarbonSpace providing the best scores. When focusing on the interannual variability of monthly anomalies and annual budgets (Figs. 8 and 14), models forced by dynamic climate data (LPJ-GUESS, SMAP-L4C and FLUXCOM) clearly outperform the CarbonSpace model, which is forced by static climate data. In particular, the SMAP-L4C provides satisfactory results, suggesting that soil moisture is a key parameter for monitoring the interannual variability of CO_2 fluxes.

Second, we show that the CO_2 flux – climate relationship is stronger for GPP and RECO than NEE and that the sign of the relationship between GPP/RECO and climate is relatively similar among the sites and products both along the annual cycle and from year-to-year (monthly anomalies and raw annual budgets). Both RECO and GPP increase when 2 m temperature, vapor pressure deficit and evapotranspiration increase and when precipitation and soil moisture decrease, in line with the literature (Haszpra et al., 2005; Tang et al., 2013; Kong et al., 2022; Li et al., 2023; Sharma et al., 2022). The NEE – climate relationship is more complex. Along the annual cycle, NEE is mainly driven by RECO during winter and GPP during summer in all datasets. From year-to-year, the magnitude of NEE anomalies is weak in most cases and their sign depends on the magnitude of the response of GPP and RECO. The latter point induces site dependencies and disagreements between observations and models and between models. From this point of view, models providing the three CO_2 fluxes (i.e., NEE, GPP and RECO) allow for a better understanding on CO_2 exchanges between the atmosphere and forest ecosystems. In addition, our study focuses on the synchronous relationship between CO_2 fluxes and individual climate parameters. Considering lead-lag relationships as well as the influence of combined climate parameters would be the next step to account for the long term effect of droughts and heatwaves on forest ecosystems (Ciais et al., 2005; von Buttlar et al., 2018). Similarly, the number of study sites was too limited to account for the influence of variable soil properties (Kurbatova et al., 2008; Besnard et al., 2018; Curtis and Gough, 2018; Martinez del Castillo et al., 2022), forest management practices (Carrara et al., 2003; Scott et al., 2004; Saunders et al., 2012) and stand age (Kurbatova et al., 2008; Besnard et al., 2018; Chuine et al., 2023).

Third, distinguishing forest stands is critical for a fine scale assessment of CO_2 temporal variability (Carrara et al., 2003, 2004; Welp et al., 2007; von Buttlar et al., 2018; Zheng et al., 2021; Kong et al., 2022). Among the models tested, the two high spatial resolution models (SMAP-L4C and CarbonSpace) distinguish forest stands, which is not the case in the 50-km resolution models (LPJ-GUESS and FLUXCOM). Our results suggest an added value of models accounting for forest stands since they are the only models to capture a clear decrease of CO_2 uptake during winter in DBF plots (Fig. 3), which is consistent with the literature (Granier et al., 2002; Welp et al., 2007). They are also the only models to capture the observed polynomial relationship between monthly 2 m temperature and NEE over the DBF plots (Fig. 7). We have, however, to acknowledge that the temporal variability of CO_2 fluxes is poorly captured in the Davos ENF site, even in the SMAP-L4C and CarbonSpace models. The main reason involves the atypical behavior of CO_2 fluxes in mountainous regions. Additional sites would be needed to

https://doi.org/10.5194/egusphere-2024-1758
Preprint. Discussion started: 20 June 2024

further understand the different responses of CO_2 fluxes to climate under DBF and ENF plots, which is out of the scope of this study.

Last, there is a hiatus in the literature regarding the emergence of trends in NEE. Some studies suggest a recent decline of CO_2 uptake by forest ecosystems in Europe (Smith et al., 2020; Thompson et al., 2020; Chuine et al., 2023; van der Woude et al., 2023), while some others suggest no trend in either the recent decade or in climate projections (Ahlström et al., 2012; Abdalla et al., 2013; Tang et al., 2013; Kong et al., 2022; Martinez del Castillo et al., 2022; Li et al., 2023). The hiatus may be explained by the location of the sites or regions under study, (ii) the limited temporal depth of observations (and models), (iii) whether or not these sites/regions have been affected by wildfires and diseases (e.g., bark beetles) and (iv) whether or not wildfires and diseases are accounted for by the models. Our results are more nuanced. We found that the evolution of the NEE annual budget does not depict any trend but that GPP and RECO may have increased recently in the observations and some models.

5 Conclusion

This study questions the strengths and limitations of state-of-the-art data-driven and process-based models to monitor and understand the temporal variability CO_2 exchanges between the atmosphere and western European temperate forest ecosystems where no flux tower measurements are available. Output from two data-driven models (CarbonSpace and FLUXCOM using different AI algorithms) and two process-based models (LPJ-GUESS and SMAP-L4C) are inter-compared over two non-instrumented sites (Châtillonnais and Mont Beuvray, France) and compared to CO_2 flux measurements from three flux tower sites (Davos, Fontainebleau and Hesse) from the FLUXNET network retained due to their proximity with the non-instrumented sites in terms of location, climate and forest stand. The focus is put on the representation of the annual cycle, annual budget, interannual variability and long-term trend in CO_2 fluxes (NEE, GPP and RECO), as well as their relationship with various climate parameters. Our results indicate that no model systematically outperforms the others. The best model in terms of representing the mean annual cycle and annual budget is not necessarily the best in capturing interannual variability. Overall, the data-driven models perform best in representing the CO_2 flux mean annual cycle and annual budget, despite considerable uncertainties from one approach to another (CarbonSpace versus FLUXCOM). As far as interannual co-variability with climate is concerned, the best performing models are those forced by dynamic instead of static climate conditions. Our results suggest that the spatial resolution of the climate drivers is likely very important in capturing spatial and temporal patterns in CO_2 exchange (e.g., in complex mountain areas). The ability to distinguish PFT spatial heterogeneity is only partially effective in representing this. Our results finally point towards the need to choose the appropriate model and spatial resolution according to the scientific question to deal with and to develop high spatial resolution models forced by dynamic climate conditions to allow for a fine scale representation of CO_2 flux temporal dynamics at the territorial level.

https://doi.org/10.5194/egusphere-2024-1758
Preprint. Discussion started: 20 June 2024

Appendices

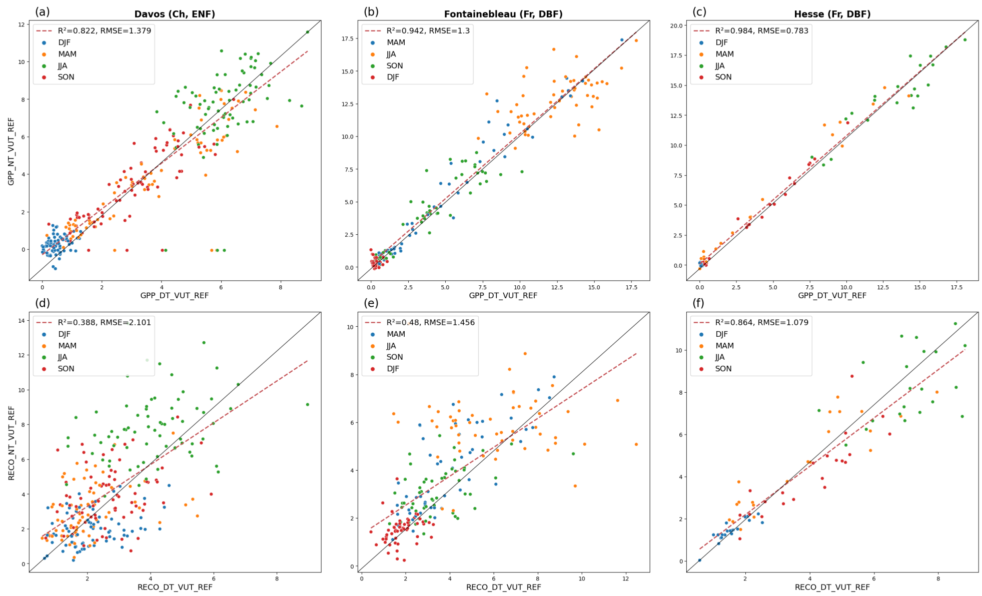

Figure A1: Comparison between (a-c) GPP and (d-f) RECO using the daytime partitioning (x-axis) and the nighttime partitioning (y-axis) for the three FLUXNET sites at the monthly timescale. The four colors correspond to the four seasons. The red line shows the linear regression between the two approaches, together with the coefficient of determination (R^2) and root mean squared error (RMSE) labeled in the insert. The black line shows the 1-by-1 correspondence.

https://doi.org/10.5194/egusphere-2024-1758
Preprint. Discussion started: 20 June 2024

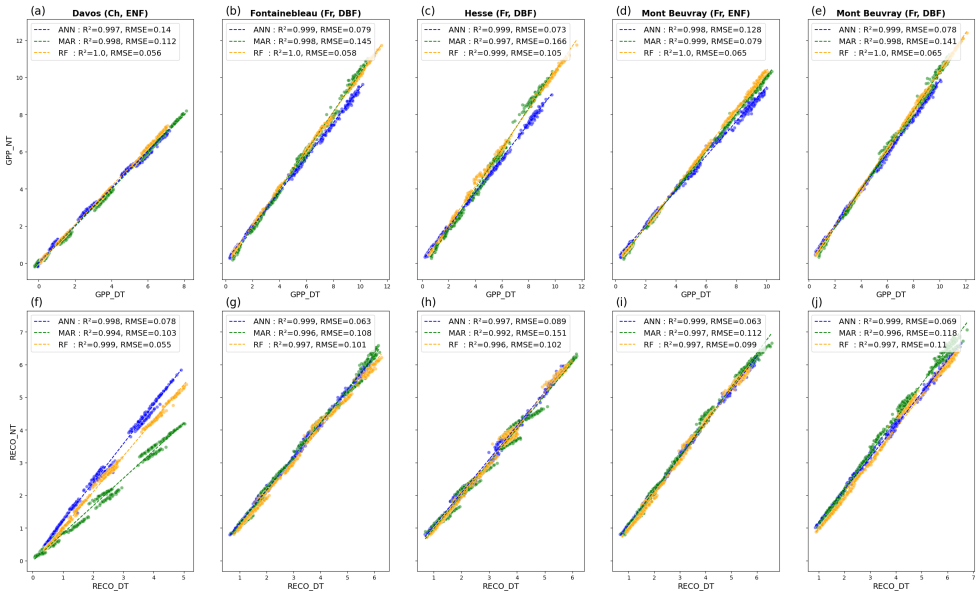

Figure A2: Comparison between FLUXCOM-simulated (a-e) GPP and (f-j) RECO using the daytime partitioning (x-axis) and the nighttime partitioning (y-axis) for the three FLUXNET sites at the monthly timescale. The three colors correspond to the three artificial intelligence algorithms. The colored lines show the linear regression between the two approaches, together with the R^2 and RMSE metrics labeled in the insert.

https://doi.org/10.5194/egusphere-2024-1758
Preprint. Discussion started: 20 June 2024

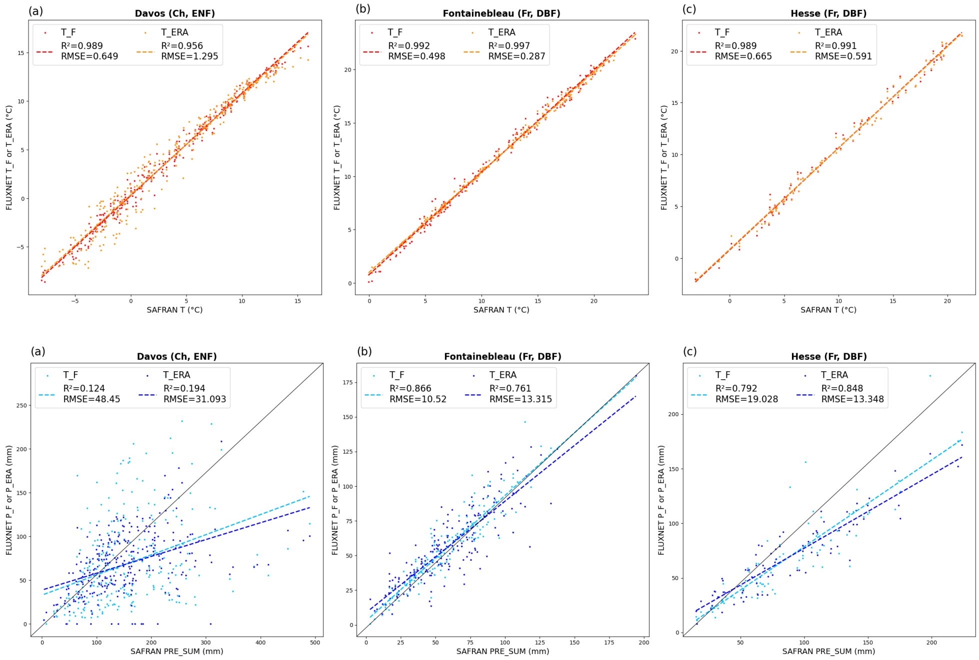

Figure A3: Comparison between the SAFRAN-SIM2 reanalysis (x-axis) and the FLUXNET observations (y-axis) for (a-c) 2 m temperature and (d-f) total precipitation for the three FLUXNET sites at the monthly timescale. The SAFRAN-SIM2 data correspond to the nearest grid point to each FLUXNET site. The SAFRAN-SIM2 – FLUXNET comparison is done using the raw and ERA-INTERIM-corrected observations, labeled T_F/P_T and T_ERA/P_ERA, respectively. The colored lines show the linear regression between the two datasets, together with the coefficient of determination (R^2) and the root mean square error (RMSE) labeled in the insert.

https://doi.org/10.5194/egusphere-2024-1758
Preprint. Discussion started: 20 June 2024

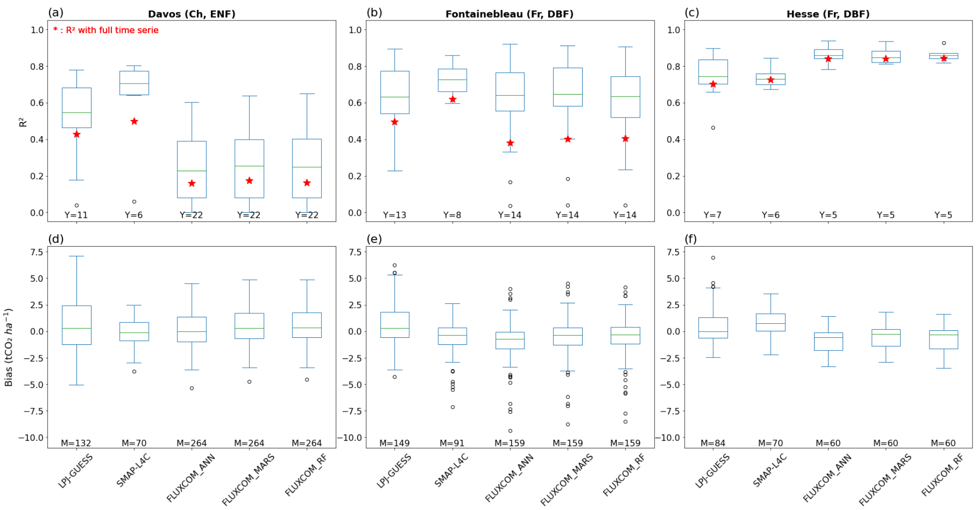

Figure A4: Same as Fig. 5 but for RECO.

https://doi.org/10.5194/egusphere-2024-1758
Preprint. Discussion started: 20 June 2024

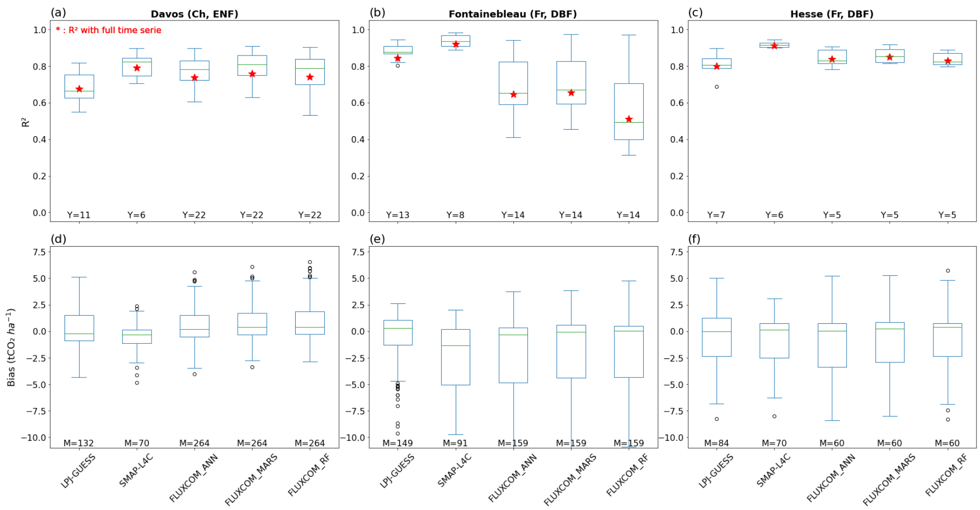

Figure A5: Same as Fig. 5 but for GPP.

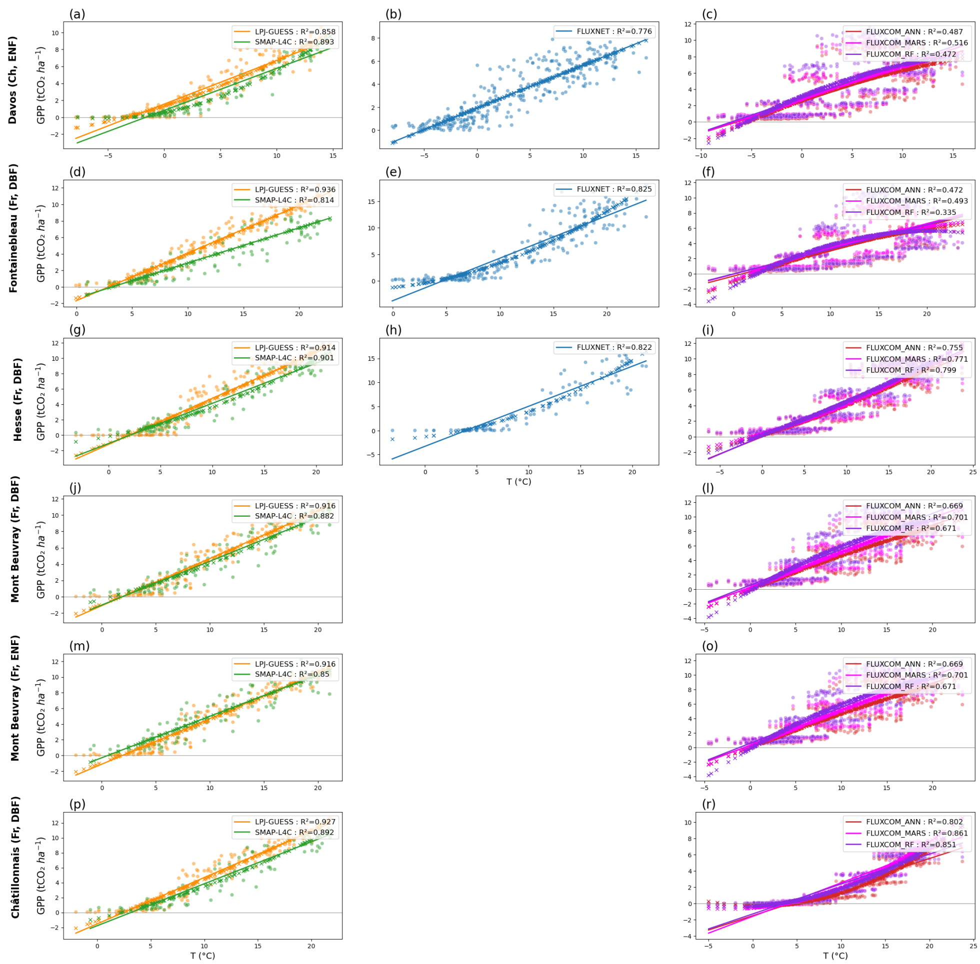

Figure A6: Same as Fig. 5 but for GPP.

https://doi.org/10.5194/egusphere-2024-1758
Preprint. Discussion started: 20 June 2024

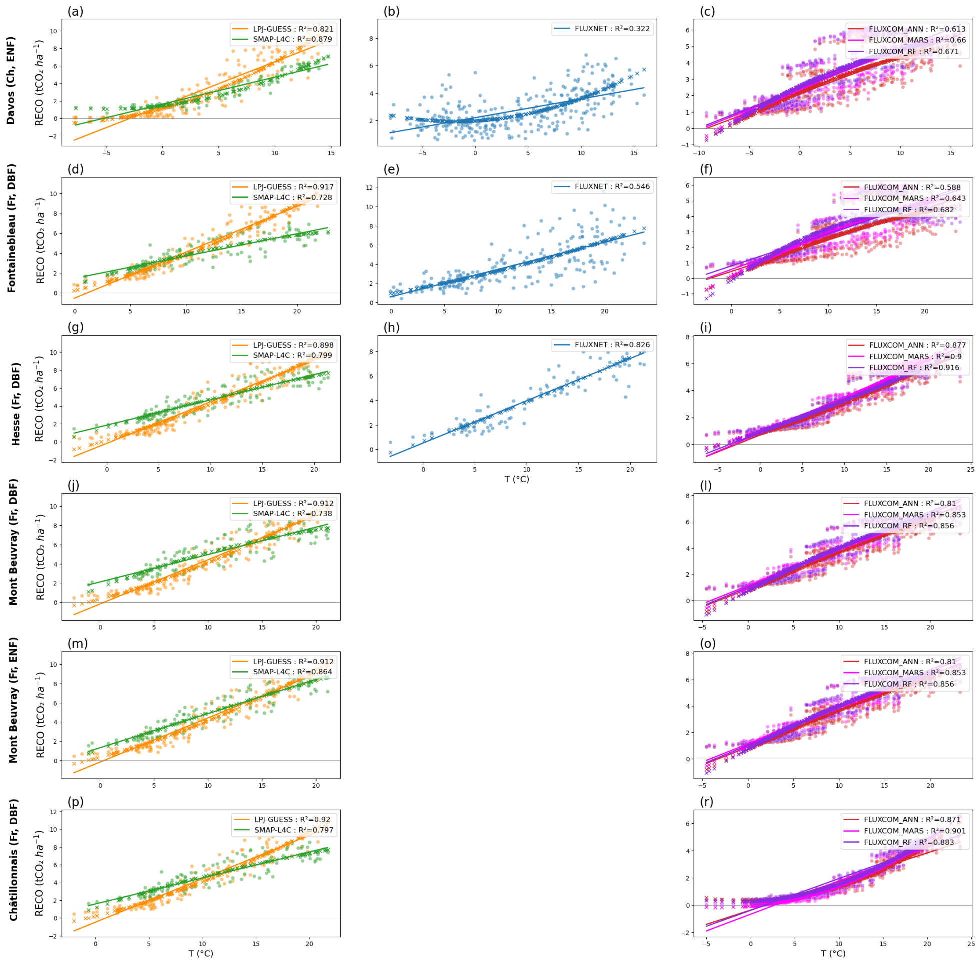

Figure A7: Same as Fig. 5 but for RECO.

https://doi.org/10.5194/egusphere-2024-1758
Preprint. Discussion started: 20 June 2024

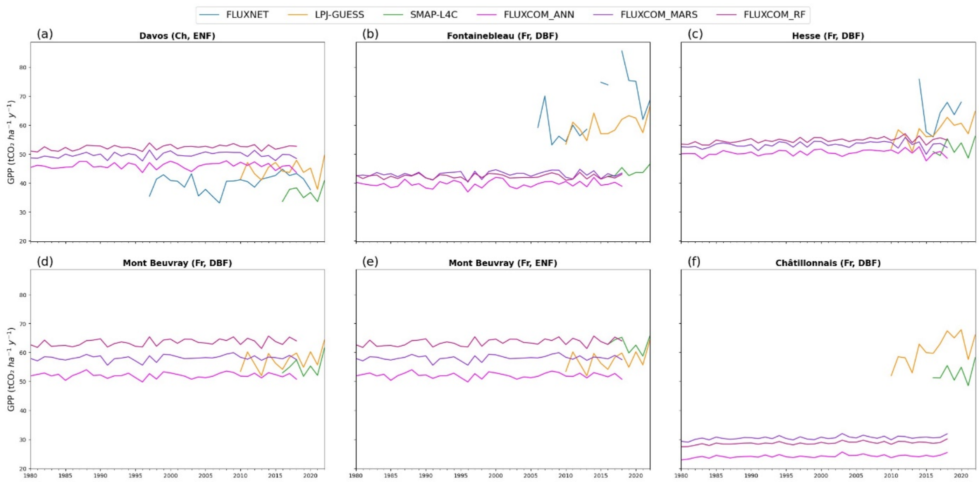

Figure A8: Same as Fig. 15 but for GPP.

https://doi.org/10.5194/egusphere-2024-1758
Preprint. Discussion started: 20 June 2024

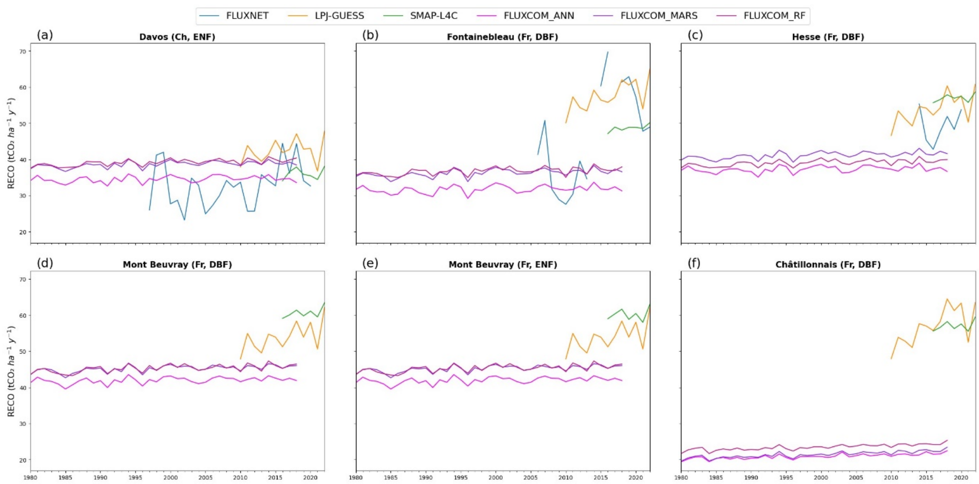

Figure A9: Same as Fig. 15 but for RECO.

https://doi.org/10.5194/egusphere-2024-1758
Preprint. Discussion started: 20 June 2024

Acknowledgement

This work is funded by the French National Research Agency (ANR-22-CPJ2-0026-01). We thank Daniel Berveiller for useful discussions on eddy covariance measurements.

Conflict of Interest

The authors declare no competing interests.

Data Availability

Climate parameters from the SAFRAN-SIM2 are available at https://meteo.data.gouv.fr. CO_2 fluxes from the FLUXOM data-driven model are available at https://www.bgc-jena.mpg.de. Those from LPJ-GUESS and SMAP-L4C process-based models are avaibable at https://meta.icos-cp.eu/collections/NZNSUglRn0VeXmGDovuVY0ec and https://nsidc.org/data/spl4cmdl/versions/7, respectively.

References

Abdalla, M., Saunders, M., Hastings, A., Williams, M., Smith, P., Osborne, B., Lanigan, G., and Jones, M. B.: Simulating the impacts of land use in Northwest Europe on Net Ecosystem Exchange (NEE): The role of arable ecosystems, grasslands and forest plantations in climate change mitigation, Sci. Total Environ., 465, 325–336, https://doi.org/10.1016/j.scitotenv.2012.12.030, 2013.

Ahlström, A., Schurgers, G., Arneth, A., and Smith, B.: Robustness and uncertainty in terrestrial ecosystem carbon response to CMIP5 climate change projections, Environ. Res. Lett., 7, 044008, https://doi.org/10.1088/1748-9326/7/4/044008, 2012.

Bayer, A. D., Pugh, T. A. M., Krause, A., and Arneth, A.: Historical and future quantification of terrestrial carbon sequestration from a Greenhouse-Gas-Value perspective, Glob. Environ. Change, 32, 153–164, https://doi.org/10.1016/j.gloenvcha.2015.03.004, 2015.

Beck, H. E., Zimmermann, N. E., McVicar, T. R., Vergopolan, N., Berg, A., and Wood, E. F.: Present and future Köppen-Geiger climate classification maps at 1-km resolution, Sci. Data, 5, 180214, https://doi.org/10.1038/sdata.2018.214, 2018.

Bergkvist, J., Lagergren, F., Linderson, M.-L. F., Miller, P., Lindeskog, M., and Jönsson, A. M.: Modelling managed forest ecosystems in Sweden: An evaluation from the stand to the regional scale, Ecol. Model., 477, 110253, https://doi.org/10.1016/j.ecolmodel.2022.110253, 2023.

Besnard, S., Carvalhais, N., Arain, M. A., Black, A., De Bruin, S., Buchmann, N., Cescatti, A., Chen, J., Clevers, J. G. P. W., Desai, A. R., Gough, C. M., Havrankova, K., Herold, M., Hörtnagl, L., Jung, M., Knohl, A., Kruijt, B., Krupkova, L., Law, B. E., Lindroth, A., Noormets, A., Roupsard, O., Steinbrecher, R., Varlagin, A., Vincke, C., and Reichstein, M.: Quantifying the effect of forest age in annual net forest carbon balance, Environ. Res. Lett., 13, 124018, https://doi.org/10.1088/1748-9326/aaeaeb, 2018.

Breiman, L.: Random Forests, Mach. Learn., 45, 5–32, https://doi.org/10.1023/A:1010933404324, 2001.

von Buttlar, J., Zscheischler, J., Rammig, A., Sippel, S., Reichstein, M., Knohl, A., Jung, M., Menzer, O., Arain, M. A., Buchmann, N., Cescatti, A., Gianelle, D., Kiely, G., Law, B. E., Magliulo, V., Margolis, H., McCaughey, H., Merbold, L., Migliavacca, M., Montagnani, L., Oechel, W., Pavelka, M., Peichl, M., Rambal, S., Raschi, A., Scott, R. L., Vaccari, F. P., van Gorsel, E., Varlagin, A., Wohlfahrt, G., and Mahecha, M. D.: Impacts of droughts and extreme-temperature events on gross primary production and ecosystem respiration: a systematic assessment across ecosystems and climate zones, Biogeosciences, 15, 1293–1318, https://doi.org/10.5194/bg-15-1293-2018, 2018.

Cai, W. and Prentice, I. C.: Recent trends in gross primary production and their drivers: analysis and modelling at flux-site and global scales, Environ. Res. Lett., 15, 124050, https://doi.org/10.1088/1748-9326/abc64e, 2020.

Carrara, A., Kowalski, A. S., Neirynck, J., Janssens, I. A., Yuste, J. C., and Ceulemans, R.: Net ecosystem CO2 exchange of mixed forest in Belgium over 5 years, Agric. For. Meteorol., 119, 209–227, https://doi.org/10.1016/S0168-1923(03)00120-5, 2003.

Carrara, A., Janssens, I. A., Curiel Yuste, J., and Ceulemans, R.: Seasonal changes in photosynthesis, respiration and NEE of a mixed temperate forest, Agric. For. Meteorol., 126, 15–31, https://doi.org/10.1016/j.agrformet.2004.05.002, 2004.

Castel, T., Lecomte, C., Richard, Y., Lejeune-Hénaut, I., and Larmure, A.: Évolution retrospective du risque gélif hivernal en climat tempéré suite au réchauffement climatique, Bourgogne-Franche-Comté Nat., 2019.

Chen, Tianqi, and Carlos Guestrin. Xgboost: A scalable tree boosting system. Proceedings of the 22nd acm sigkdd international conference on knowledge discovery and data mining, 785-794. 2016.

Chuine, I., Ciais, P., Cramer, W., and Laskar, J.: Les forêts françaises face au changement climatique. Rapport du Comité des sciences de l'environnement de l'Académie des sciences et points de vue d'Académiciens de l'Académie d'Agriculture de France., Comité des sciences de l'environnement de l'Académie des sciences, 2023.

Curtis, P. S. and Gough, C. M.: Forest aging, disturbance and the carbon cycle, New Phytol., 219, 1188–1193, https://doi.org/10.1111/nph.15227, 2018.

Endsley, K. A., Kimball, J. S., Kundig, T., Reichle, R. H., and Ardizzone, J. V.: Validation Assessment for the Soil Moisture Active Passive (SMAP) Level 4 Carbon (L4_C) Data Product Version 7, 2023.

Friedman, J. H.: Multivariate Adaptive Regression Splines, Ann. Stat., 19, 1–67, https://doi.org/10.1214/aos/1176347963, 1991.

Hardouin, L., Delire, C., Decharme, B., Lawrence, D. M., Nabel, J. E. M. S., Brovkin, V., Collier, N., Fisher, R., Hoffman, F. M., Koven, C. D., Séférian, R., and Stacke, T.: Uncertainty in land carbon budget simulated by terrestrial biosphere models: the role of atmospheric forcing, Environ. Res. Lett., 17, 094033, https://doi.org/10.1088/1748-9326/ac888d, 2022.

He, B., Chen, C., Lin, S., Yuan, W., Chen, H. W., Chen, D., Zhang, Y., Guo, L., Zhao, X., Liu, X., Piao, S., Zhong, Z., Wang, R., and Tang, R.: Worldwide impacts of atmospheric vapor pressure deficit on the interannual variability of terrestrial carbon sinks, Natl. Sci. Rev., 9, nwab150, https://doi.org/10.1093/nsr/nwab150, 2022.

Hersbach, H., Bell, B., Berrisford, P., Hirahara, S., Horányi, A., Muñoz-Sabater, J., Nicolas, J., Peubey, C., Radu, R., Schepers, D., Simmons, A., Soci, C., Abdalla, S., Abellan, X., Balsamo, G., Bechtold, P., Biavati, G., Bidlot, J., Bonavita, M., De Chiara, G., Dahlgren, P., Dee, D., Diamantakis, M., Dragani, R., Flemming, J., Forbes, R., Fuentes, M., Geer, A., Haimberger, L., Healy, S., Hogan, R. J., Hólm, E., Janisková, M., Keeley, S., Laloyaux, P., Lopez, P., Lupu, C., Radnoti, G., de Rosnay, P., Rozum, I., Vamborg, F., Villaume, S., and Thépaut, J.-N.: The ERA5 global reanalysis, Q. J. R. Meteorol. Soc., 146, 1999–2049, https://doi.org/10.1002/qj.3803, 2020.

https://doi.org/10.5194/egusphere-2024-1758
Preprint. Discussion started: 20 June 2024

IGN: Inventaire Forestier National ; Mémento édition 2022, 2022.

IPCC: Climate Change 2022 – Impacts, Adaptation and Vulnerability: Working Group II Contribution to the Sixth Assessment Report of the Intergovernmental Panel on Climate Change, 1st ed., Cambridge University Press, https://doi.org/10.1017/9781009325844, 2023.

Jones, L. A., Kimball, J. S., Reichle, R. H., Madani, N., Glassy, J., Ardizzone, J. V., Colliander, A., Cleverly, J., Desai, A. R., Eamus, D., Euskirchen, E. S., Hutley, L., Macfarlane, C., and Scott, R. L.: The SMAP Level 4 Carbon Product for Monitoring Ecosystem Land–Atmosphere CO_2 Exchange, IEEE Trans. Geosci. Remote Sens., 55, 6517–6532, https://doi.org/10.1109/TGRS.2017.2729343, 2017.

Jung, M., Koirala, S., Weber, U., Ichii, K., Gans, F., Camps-Valls, G., Papale, D., Schwalm, C., Tramontana, G., and Reichstein, M.: The FLUXCOM ensemble of global land-atmosphere energy fluxes, Sci. Data, 6, 74, https://doi.org/10.1038/s41597-019-0076-8, 2019.

Jung, M., Schwalm, C., Migliavacca, M., Walther, S., Camps-Valls, G., Koirala, S., Anthoni, P., Besnard, S., Bodesheim, P., Carvalhais, N., Chevallier, F., Gans, F., Goll, D. S., Haverd, V., Köhler, P., Ichii, K., Jain, A. K., Liu, J., Lombardozzi, D., Nabel, J. E. M. S., Nelson, J. A., O'Sullivan, M., Pallandt, M., Papale, D., Peters, W., Pongratz, J., Rödenbeck, C., Sitch, S., Tramontana, G., Walker, A., Weber, U., and Reichstein, M.: Scaling carbon fluxes from eddy covariance sites to globe: synthesis and evaluation of the FLUXCOM approach, Biogeosciences, 17, 1343–1365, https://doi.org/10.5194/bg-17-1343-2020, 2020.

Kimball, J. S., Jones, L. A., Endsley, A., Kundig, T., and Reichle, R.: SMAP L4 Global Daily 9 km EASE-Grid Carbon Net Ecosystem Exchange, Version 7 User Guide, https://doi.org/10.5067/3K9F0S1Q5J2U, 2022.

Kong, Z., Wang, T., Han, Q., Dai, Y., Wang, L., and Chen, X.: Evaluation of Environmental Controls on Terrestrial Net Ecosystem Exchange of CO_2: A Global Perspective From the FLUXNET Sites, J. Geophys. Res. Atmospheres, 127, e2022JD037217, https://doi.org/10.1029/2022JD037217, 2022.

Kurbatova, J., Li, C., Varlagin, A., Xiao, X., and Vygodskaya, N.: Modeling carbon dynamics in two adjacent spruce forests with different soil conditions in Russia, 2008.

Lasslop, G., Reichstein, M., Papale, D., Richardson, A. D., Arneth, A., Barr, A., Stoy, P., and Wohlfahrt, G.: Separation of net ecosystem exchange into assimilation and respiration using a light response curve approach: critical issues and global evaluation, Glob. Change Biol., 16, 187–208, https://doi.org/10.1111/j.1365-2486.2009.02041.x, 2010.

Le Quéré, C., Andrew, R. M., Friedlingstein, P., Sitch, S., Pongratz, J., Manning, A. C., Korsbakken, J. I., Peters, G. P., Canadell, J. G., Jackson, R. B., Boden, T. A., Tans, P. P., Andrews, O. D., Arora, V. K., Bakker, D. C. E., Barbero, L., Becker, M., Betts, R. A., Bopp, L., Chevallier, F., Chini, L. P., Ciais, P., Cosca, C. E., Cross, J., Currie, K., Gasser, T., Harris, I., Hauck, J., Haverd, V., Houghton, R. A., Hunt, C. W., Hurtt, G., Ilyina, T., Jain, A. K., Kato, E., Kautz, M., Keeling, R. F., Klein Goldewijk, K., Körtzinger, A., Landschützer, P., Lefèvre, N., Lenton, A., Lienert, S., Lima, I., Lombardozzi, D., Metzl, N., Millero, F., Monteiro, P. M. S., Munro, D. R., Nabel, J. E. M. S., Nakaoka, S., Nojiri, Y., Padin, X. A., Peregon, A., Pfeil, B., Pierrot, D., Poulter, B., Rehder, G., Reimer, J., Rödenbeck, C., Schwinger, J., Séférian, R., Skjelvan, I., Stocker, B. D., Tian, H., Tilbrook, B., Tubiello, F. N., van der Laan-Luijkx, I. T., van der Werf, G. R., van Heuven, S., Viovy, N., Vuichard, N., Walker, A. P., Watson, A. J., Wiltshire, A. J., Zaehle, S., and Zhu, D.: Global Carbon Budget 2017, Earth Syst. Sci. Data, 10, 405–448, https://doi.org/10.5194/essd-10-405-2018, 2018.

Li, Q., Tietema, A., Reinsch, S., Schmidt, I. K., de Dato, G., Guidolotti, G., Lellei-Kovács, E., Kopittke, G., and Larsen, K. S.: Higher sensitivity of gross primary productivity than ecosystem respiration to experimental drought and warming across six European shrubland ecosystems, Sci. Total Environ., 900, 165627, https://doi.org/10.1016/j.scitotenv.2023.165627, 2023.

Lindeskog, M., Smith, B., Lagergren, F., Sycheva, E., Ficko, A., Pretzsch, H., and Rammig, A.: Accounting for forest management in the estimation of forest carbon balance using the dynamic vegetation model LPJ-GUESS (v4.0, r9710): implementation and evaluation of simulations for Europe, Geosci. Model Dev., 14, 6071–6112, https://doi.org/10.5194/gmd-14-6071-2021, 2021.

https://doi.org/10.5194/egusphere-2024-1758
Preprint. Discussion started: 20 June 2024

Martinez del Castillo, E., Zang, C. S., Buras, A., Hacket-Pain, A., Esper, J., Serrano-Notivoli, R., Hartl, C., Weigel, R., Klesse, S., Resco de Dios, V., Scharnweber, T., Dorado-Liñán, I., van der Maaten-Theunissen, M., van der Maaten, E., Jump, A., Mikac, S., Banzragch, B.-E., Beck, W., Cavin, L., Claessens, H., Čada, V., Čufar, K., Dulamsuren, C., Gričar, J., Gil-Pelegrín, E., Janda, P., Kazimirovic, M., Kreyling, J., Latte, N., Leuschner, C., Longares, L. A., Menzel, A., Merela, M., Motta, R., Muffler, L., Nola, P., Petritan, A. M., Petritan, I. C., Prislan, P., Rubio-Cuadrado, Á., Rydval, M., Stajić, B., Svoboda, M., Toromani, E., Trotsiuk, V., Wilmking, M., Zlatanov, T., and de Luis, M.: Climate-change-driven growth decline of European beech forests, Commun. Biol., 5, 1–9, https://doi.org/10.1038/s42003-022-03107-3, 2022.

McKnight, P. E. and Najab, J.: Mann-Whitney U Test, in: The Corsini Encyclopedia of Psychology, John Wiley & Sons, Ltd, 1–1, https://doi.org/10.1002/9780470479216.corpsy0524, 2010.

Menzel, A., Yuan, Y., Matiu, M., Sparks, T., Scheifinger, H., Gehrig, R., and Estrella, N.: Climate change fingerprints in recent European plant phenology, Glob. Change Biol., 26, 2599–2612, https://doi.org/10.1111/gcb.15000, 2020.

Monteith, J. and Unsworth, M.: Principles of Environmental Physics - 3rd Edition, Academic Press, 440 pp., 2007.

Muñoz-Sabater, J., Dutra, E., Agustí-Panareda, A., Albergel, C., Arduini, G., Balsamo, G., Boussetta, S., Choulga, M., Harrigan, S., Hersbach, H., Martens, B., Miralles, D. G., Piles, M., Rodríguez-Fernández, N. J., Zsoter, E., Buontempo, C., and Thépaut, J.-N.: ERA5-Land: a state-of-the-art global reanalysis dataset for land applications, Earth Syst. Sci. Data, 13, 4349–4383, https://doi.org/10.5194/essd-13-4349-2021, 2021.

Pan, Y., Birdsey, R. A., Fang, J., Houghton, R., Kauppi, P. E., Kurz, W. A., Phillips, O. L., Shvidenko, A., Lewis, S. L., Canadell, J. G., Ciais, P., Jackson, R. B., Pacala, S. W., McGuire, A. D., Piao, S., Rautiainen, A., Sitch, S., and Hayes, D.: A Large and Persistent Carbon Sink in the World's Forests, Science, 333, 988–993, https://doi.org/10.1126/science.1201609, 2011.

Papale, D. and Valentini, R.: A new assessment of European forests carbon exchanges by eddy fluxes and artificial neural network spatialization, Glob. Change Biol., 9, 525–535, https://doi.org/10.1046/j.1365-2486.2003.00609.x, 2003.

Prislan, P., Gričar, J., Čufar, K., de Luis, M., Merela, M., and Rossi, S.: Growing season and radial growth predicted for Fagus sylvatica under climate change, Clim. Change, 153, 181–197, https://doi.org/10.1007/s10584-019-02374-0, 2019.

Pugh, T. A. M., Lindeskog, M., Smith, B., Poulter, B., Arneth, A., Haverd, V., and Calle, L.: Role of forest regrowth in global carbon sink dynamics, Proc. Natl. Acad. Sci., 116, 4382–4387, https://doi.org/10.1073/pnas.1810512116, 2019.

Sathyanadh, A., Monteil, G., Scholze, M., Klosterhalfen, A., Laudon, H., Wu, Z., Gerbig, C., Peters, W., Bastrikov, V., Nilsson, M. B., and Peichl, M.: Reconciling the Carbon Balance of Northern Sweden Through Integration of Observations and Modelling, J. Geophys. Res. Atmospheres, 126, e2021JD035185, https://doi.org/10.1029/2021JD035185, 2021.

Sharma, B., Kumar, J., Collier, N., Ganguly, A. R., and Hoffman, F. M.: Quantifying Carbon Cycle Extremes and Attributing Their Causes Under Climate and Land Use and Land Cover Change From 1850 to 2300, Journal of Geophysical Research: Biogeosciences, 127, e2021JG006738, https://doi.org/10.1029/2021JG006738, 2022.

Smith, B., Prentice, I. C., and Sykes, M. T.: Representation of vegetation dynamics in the modelling of terrestrial ecosystems: comparing two contrasting approaches within European climate space, Glob. Ecol. Biogeogr., 10, 621–637, https://doi.org/10.1046/j.1466-822X.2001.t01-1-00256.x, 2001.

Smith, B., Wårlind, D., Arneth, A., Hickler, T., Leadley, P., Siltberg, J., and Zaehle, S.: Implications of incorporating N cycling and N limitations on primary production in an individual-based dynamic vegetation model, Biogeosciences, 11, 2027–2054, https://doi.org/10.5194/bg-11-2027-2014, 2014.

Soubeyroux, J.-M., Martin, E., Franchisteguy, L., Habets, F., Noilhan, J., BAILLON, M., Rousset, F., Vidal, J.-P., LEMOIGNE, P., and Morel, S.: Safran-Isba-Modcou (SIM) : Un outil pour le suivi hydrométéorologique opérationnel et les études, La Météorologie, 40–45, https://doi.org/10.4267/2042/21890, 2008.

https://doi.org/10.5194/egusphere-2024-1758
Preprint. Discussion started: 20 June 2024

Tang, X., Wang, Z., Xie, J., Liu, D., Desai, A. R., Jia, M., Dong, Z., Liu, X., and Liu, B.: Monitoring the seasonal and interannual variation of the carbon sequestration in a temperate deciduous forest with MODIS time series data, For. Ecol. Manag., 306, 150–160, https://doi.org/10.1016/j.foreco.2013.06.032, 2013.

Tramontana, G., Jung, M., Schwalm, C. R., Ichii, K., Camps-Valls, G., Ráduly, B., Reichstein, M., Arain, M. A., Cescatti, A., Kiely, G., Merbold, L., Serrano-Ortiz, P., Sickert, S., Wolf, S., and Papale, D.: Predicting carbon dioxide and energy fluxes across global FLUXNET sites with regression algorithms, Biogeosciences, 13, 4291–4313, https://doi.org/10.5194/bg-13-4291-2016, 2016.

Valentini, R., Arneth, A., Bombelli, A., Castaldi, S., Cazzolla Gatti, R., Chevallier, F., Ciais, P., Grieco, E., Hartmann, J., Henry, M., Houghton, R. A., Jung, M., Kutsch, W. L., Malhi, Y., Mayorga, E., Merbold, L., Murray-Tortarolo, G., Papale, D., Peylin, P., Poulter, B., Raymond, P. A., Santini, M., Sitch, S., Vaglio Laurin, G., van der Werf, G. R., Williams, C. A., and Scholes, R. J.: A full greenhouse gases budget of Africa: synthesis, uncertainties, and vulnerabilities, Biogeosciences, 11, 381–407, https://doi.org/10.5194/bg-11-381-2014, 2014.

Walker, A. P., De Kauwe, M. G., Bastos, A., Belmecheri, S., Georgiou, K., Keeling, R. F., McMahon, S. M., Medlyn, B. E., Moore, D. J. P., Norby, R. J., Zaehle, S., Anderson-Teixeira, K. J., Battipaglia, G., Brienen, R. J. W., Cabugao, K. G., Cailleret, M., Campbell, E., Canadell, J. G., Ciais, P., Craig, M. E., Ellsworth, D. S., Farquhar, G. D., Fatichi, S., Fisher, J. B., Frank, D. C., Graven, H., Gu, L., Haverd, V., Heilman, K., Heimann, M., Hungate, B. A., Iversen, C. M., Joos, F., Jiang, M., Keenan, T. F., Knauer, J., Körner, C., Leshyk, V. O., Leuzinger, S., Liu, Y., MacBean, N., Malhi, Y., McVicar, T. R., Penuelas, J., Pongratz, J., Powell, A. S., Riutta, T., Sabot, M. E. B., Schleucher, J., Sitch, S., Smith, W. K., Sulman, B., Taylor, B., Terrer, C., Torn, M. S., Treseder, K. K., Trugman, A. T., Trumbore, S. E., van Mantgem, P. J., Voelker, S. L., Whelan, M. E., and Zuidema, P. A.: Integrating the evidence for a terrestrial carbon sink caused by increasing atmospheric CO2, New Phytol., 229, 2413–2445, https://doi.org/10.1111/nph.16866, 2020.

Warm Winter 2020 Team and ICOS Ecosystem Thematic Centre: Warm Winter 2020 ecosystem eddy covariance flux product for 73 stations in FLUXNET-Archive format—release 2022-1, https://doi.org/10.18160/2G60-ZHAK, 2022.

Welp, L. R., Randerson, J. T., and Liu, H. P.: The sensitivity of carbon fluxes to spring warming and summer drought depends on plant functional type in boreal forest ecosystems, Agric. For. Meteorol., 147, 172–185, https://doi.org/10.1016/j.agrformet.2007.07.010, 2007.

van der Woude, A. M., Peters, W., Joetzjer, E., Lafont, S., Koren, G., Ciais, P., Ramonet, M., Xu, Y., Bastos, A., Botía, S., Sitch, S., de Kok, R., Kneuer, T., Kubistin, D., Jacotot, A., Loubet, B., Herig-Coimbra, P.-H., Loustau, D., and Luijkx, I. T.: Temperature extremes of 2022 reduced carbon uptake by forests in Europe, Nat. Commun., 14, 6218, https://doi.org/10.1038/s41467-023-41851-0, 2023.

Wu, Z., Ahlström, A., Smith, B., Ardö, J., Eklundh, L., Fensholt, R., and Lehsten, V.: Climate data induced uncertainty in model-based estimations of terrestrial primary productivity, Environ. Res. Lett., 12, 064013, https://doi.org/10.1088/1748-9326/aa6fd8, 2017.

Zheng, P., Wang, D., Yu, X., Jia, G., Liu, Z., Wang, Y., and Zhang, Y.: Effects of drought and rainfall events on soil autotrophic respiration and heterotrophic respiration, Agric. Ecosyst. Environ., 308, 107267, https://doi.org/10.1016/j.agee.2020.107267, 2021.

Zhuravlev, R., Dara, A., Santos, A. L. D. dos, Demidov, O., and Burba, G.: Globally Scalable Approach to Estimate Net Ecosystem Exchange Based on Remote Sensing, Meteorological Data, and Direct Measurements of Eddy Covariance Sites, Remote Sens., 14, 5529, https://doi.org/10.3390/rs14215529, 2022.